

# Investigation of Nuclear Phase Transition by Solvababe supersymmetric algebraic model and its application in Ru-Rh and Zn-Cu Isotopes

M. A. Jafarizadeh\*

*Department of Theoretical Physics and Astrophysics, University of Tabriz, Tabriz 51664, Iran. and  
Research Institute for Fundamental Sciences, Tabriz 51664, Iran*

M.Ghapanvari†

*Department of Nuclear Physics, University of Tabriz, Tabriz 51664, Iran. and  
The Plasma Physics and Fusion Research School, Tehran, Iran.*

N.Fouladi‡ and Z.Ranjbar§

*Department of Nuclear Physics, University of Tabriz, Tabriz 51664, Iran.*

A.Sadighzadeh

*The Plasma Physics and Fusion Research School, Tehran, Iran.*

(Dated: July 3, 2021)

Solvable supersymmetric algebraic model for descriptions of the spherical to  $\gamma$  - *unstable* shape-phase transition in even and odd mass nuclei is proposed. This model is based on dual algebraic structure and Richardson - Gaudin method, where the duality relations between the unitary and quasispin algebraic structures for the boson and fermion systems are extended to mixed boson-fermion system. The structure of two type of nuclear supersymmetry schemes, based on the  $U(6/2)$  and  $U(6/4)$  supergroups, is discussed. We investigate the change in level structure induced by the phase transition by doing a quantal analysis. By using the generalized quasispin algebra, it is shown that the nuclear supersymmetry concept can be also used for transitional regions in addition to dynamical symmetry limits. Experimental evidence for the  $U(5)$ - $O(6)$  transition in Ru-Rh and Zn-Cu supermultiplets is presented. The low-states energy spectra and  $B(E2)$  values for these nuclei have been calculated and compared with the experimental data.

arXiv:1602.06849v1 [nucl-th] 7 Dec 2015

---

\* jafarizadeh@tabrizu.ac.ir

† M.ghapanvari@tabrizu.ac.ir

‡ fooladi@tabrizu.ac.ir

§ Z.ranjbar@tabrizu.ac.ir

## I. INTRODUCTION

Symmetry is one of the fundamental concepts in physics. In the nuclei, symmetry is in the form of dynamical symmetry. The dynamical symmetries were introduced in nuclear physics with the development of the interacting boson model and its extensions[1, 2]. The IBM describes the collective excitations of even-even nuclei in terms of correlated pairs of nucleons with  $L = 0, 2$  treated as bosons (s, d bosons)[1]. The IBM represents a simple description of nuclear collective excitations based of an algebraic theory where symmetry transformations play a significant role. The N-boson system space is spanned by the irrep  $[N]$  of  $U^B(6)$  [1]. The interacting boson - fermion model also explains odd-A nuclei in terms of correlated pairs, s and d bosons, and unpaired particles of angular momentum  $j$  ( $j$  fermions)[2]. The states of the boson - fermion system can be classified according to the irreducible representation  $[N] \times [1]$  of  $U^B(6) \times U^F(M)$  where  $M$  is the dimension of the single particle space. The IBM and IBFM can be unified into a supersymmetry (SUSY) approach that was discovered into nuclear structure physics in the early 1980 [3, 4]. The experiments performed at various laboratories have confirmed the predictions made using a SUSY scheme [5]. Originally, nuclear supersymmetry was considered as symmetry among pairs of nuclei consisting of an even-even and an odd-even nucleus[3, 4]. The supersymmetric representations  $[\mathcal{N}]$ ,  $\mathcal{N} = N_B + N_F$ , of  $U(6/M)$  spanned a space that explains the lowest states of an even-even nucleus with  $\mathcal{N}$  bosons and an odd-A nucleus with  $\mathcal{N} - 1$  bosons and a unpaired fermion[2]. In supersymmetry approach, the core-particle interaction entirely are determined by the even-even Hamiltonian and most of the parameters in the core-particle interaction can be taken from the neighboring even-even nucleus thus the nuclear properties of neighboring even-even and odd-A nuclei can be described with a single Hamiltonian and a single set of transition and transfer operators[2, 6]. The nuclear supersymmetry have been used successfully in description dynamical symmetry limits of the even-even and odd-A nuclei[2-4, 7]. The IBFM could be an ideal ground for testing supersymmetry[7]. Virtually simultaneously, with the introduction of the nuclear supersymmetry, the idea of spherical-deformed phase transitions at low energy in finite nuclei germinated[8, 9]. Studies of QPTs in odd-even nuclei with supersymmetric scheme had implicitly been initiated years before by A. Frank et al.[6]. They have studied successfully a combination of  $U^{BF}(5)$  and  $SO^{BF}(6)$  symmetry by using  $U(6/12)$  supersymmetry for the Ru and Rh isotopes. Iachello [10] extended the concept of critical symmetry to critical supersymmetry and provided a benchmark for the study of shape phase transition in odd-even nuclei and also J.Jolie et al.[11] studied QPTs in odd-even nuclei using a supersymmetric approach in interacting Boson-Fermion model.

In this paper, concept of supersymmetry and phase transitions are brought together by using the generalized quasi-spin algebra and Richardson - Gaudin method. Exactly solvable solution for the spherical to gamma - unstable transition in transitional nuclei based on dual algebraic structure and nuclear supersymmetry concept is proposed. Two separate cases are considered with the fermions lying in a  $j=1/2$  shell or in a  $j=3/2$  shell. The existence of duality symmetries has proven to be a powerful tool in relating the Hamiltonians with the number-conserving unitary and number-nonconserving quasispin algebras for system with pairing interactions that first introduced in nuclear physics in Ref.[12] and further developed in Refs.[13, 14]. These relations were obtained for both bosonic and fermionic systems[13, 14]. We have established the duality relations for mixed boson-fermion system. We evaluate exact solutions for eigenstate and energy eigenvalues for transitional region and dynamical-symmetry limits for even-even and odd-A nuclei in Supersymmetry scheme by using Richardson - Gaudin method and changing the control parameters that based on affine  $\widehat{GQA}$  generalized quasi-spin algebra. In order to investigation of phase transition, we calculate observables such as level crossing, expectation values of the d-boson number operator and expectation values of the fermion number operator. The low-lying states of even-mass ruthenium and the odd-mass rhodium isotopes and Zn-Cu supermultiplets have been studied within suggested model. The results of calculations for these nuclei will present for energy levels and transitions probabilities, two neutron separation energies and will compare with the corresponding the experimental data.

This paper is organized as follows: Section 2 briefly summarizes theoretical aspects of transitional Hamiltonian and generalized quasi-spin algebraic technique. Sections 3 and 4 include the quantal analysis and experimental evidence and sect. 5 is devoted to the summary and some conclusions.

## II. THEORETICAL FRAMEWORK

### A. The Model

The quasispin algebras have been explained in detail in Refs [12-14]. The  $SU(1,1)$  algebra is produced by  $S^\nu$ ,  $\nu = 0$  and  $\pm$ , which satisfies the following commutation relations[12-14]

$$[S_B^0, S_B^\pm] = \pm S_B^\pm \quad , \quad [S_B^+, S_B^-] = -2S_B^0 \quad (1)$$

In IBM , the generators of  $SU^d(1, 1)$  generated by the d-boson pairing algebra[12]

$$S^+(d) = \frac{1}{2}(d^+ \cdot d^+) \quad , \quad S^-(d) = \frac{1}{2}(\tilde{d} \cdot \tilde{d}), \quad S^0(d) = \frac{1}{4} \sum_{\nu} (d_{\nu}^+ d_{\nu} + d_{\nu} d_{\nu}^+) = \frac{1}{4}(2\hat{n}_d + 5) \quad (2)$$

Similarly, s- boson pairing algebra forms another  $SU^s(1, 1)$  algebra generated by [12]

$$S^+(s) = \frac{1}{2}s^{+2} \quad , \quad S^-(s) = \frac{1}{2}s^2, \quad S^0(s) = \frac{1}{4}(s^+ s + s s^+) = \frac{1}{4}(2\hat{n}_s + 1) \quad (3)$$

$SU^{sd}(1, 1)$  is the s and d boson pairing algebras generated by[12]

$$S^+(sd) = \frac{1}{2}(d^+ \cdot d^+ \pm s^{+2}) \quad , \quad S^-(sd) = \frac{1}{2}(\tilde{d} \cdot \tilde{d} \pm s^2) \quad , \quad S^0(sd) = \frac{1}{4} \sum_{\nu} (d_{\nu}^+ d_{\nu} + d_{\nu} d_{\nu}^+) + \frac{1}{4}(s^+ s + s s^+) \quad (4)$$

The fermionic quasispin operators are[13, 14]

$$S_F^+ = \frac{1}{2} \sum_{m'} (-1)^{j \mp m'} a_{jm'}^+ a_{j-m'}^+ = \frac{1}{2}(a_j^+ \cdot a_j^+) \quad (5)$$

$$S_F^- = \frac{1}{2} \sum_{m'} (-1)^{j \mp m'} \tilde{a}_{jm'} \tilde{a}_{j-m'} = \frac{1}{2}(\tilde{a}_j \cdot \tilde{a}_j) \quad (6)$$

$$S_F^0 = \frac{n_f}{2} - \frac{2j+1}{4} \quad (7)$$

satisfy the commutation relations of the fermion quasispin  $SU(2)$  algebra[13, 14].

$$[S_F^0, S_F^{\pm}] = \pm S_F^{\pm} \quad , \quad [S_F^+, S_F^-] = 2S_F^0 \quad (8)$$

The generalized quasispin algebra contain both bosonic (B) and fermionic (F) operators defined as [15]

$$S_{BF}^0 = S_B^0 + S_F^0, \quad S_{BF}^+ = S_B^+ + S_F^+, \quad S_{BF}^- = S_B^- + S_F^- \quad (9)$$

Thus

$$S_{BF}^0 = \frac{1}{4}(N - M) + \frac{1}{2}(n_b + n_f) \quad (10)$$

$$S_{BF}^+ = \frac{1}{2} \sum_m (-1)^{2 \mp m} b_m^+ b_{-m}^+ \mp \frac{1}{2} \sum_{m'} (-1)^{j \mp m'} a_{jm'}^+ a_{j-m'}^+ = \frac{1}{2}(b^+ \cdot b^+) \mp (a_j^+ \cdot a_j^+) \quad (11)$$

$$S_{BF}^- = \frac{1}{2}(\tilde{b} \cdot \tilde{b}) \pm \frac{1}{2}(\tilde{a}_j \cdot \tilde{a}_j) \quad (12)$$

Where  $n_b$  and  $n_f$  are the boson and fermion number operator, respectively. Thus the operators  $(S_{BF}^{\pm}, S_{BF}^0)$  form a generalization of the usual fermionic and bosonic quasispin algebras with commutation relations given as[15]

$$[S_{BF}^0, S_{BF}^{\pm}] = \pm S_{BF}^{\pm} \quad , \quad [S_{BF}^+, S_{BF}^-] = -2S_{BF}^0 \quad (13)$$

The generalized quasispin algebra(GQA) may be labeled in terms of the eigenvalues of the second-order Casimir invariant and those of the quasispin operator  $S_{BF}^0$  [15]. The second-order Casimir invariant for the GQA is defined as

$$C_2(GQA) = S_{BF}^0(S_{BF}^0 - 1) - S_{BF}^+ S_{BF}^- \quad (14)$$

The basis states of an irreducible representation (irrep)GQA,  $|k, \mu\rangle$ , are determined by a single number  $k$ , where can be any positive number and  $\mu = k, k+1, \dots$ . Therefore,

$$S_{BF}^0 |k, \mu\rangle = \left( \frac{N-M}{4} + \frac{(N_B + N_F)}{2} \right) |k, \mu\rangle \quad (15)$$

$$C_2(su(1,1))|k, \mu\rangle = k(k-1)|k, \mu\rangle = \left(\frac{N-M}{4} + \frac{(\nu_B + \nu_F)}{2}\right)\left(\frac{N-M}{4} + \frac{(\nu_B + \nu_F)}{2} - 1\right)|k, \mu\rangle \quad (16)$$

$$|k, \mu\rangle = \left|\frac{N-M}{4} + \frac{\nu_B + \nu_F}{2}, \frac{N-M}{4} + \frac{N_B + N_F}{2}\right\rangle \quad (17)$$

The basis states are determined considering the fact that fermionic part of the action of  $S_{BF}^+$  is restricted by the Pauli Exclusion Principle and the action of  $S_{BF}^-$  terminates when a state of  $\nu$  unpaired particles is reached i.e  $S_{BF}^-|\nu_B, \nu_F\rangle = 0$  [15].

The infinite dimensional generalized quasispin algebra that is generated by use of [12]

$$S_{BF,n}^\pm = c_s^{2n+1}S_B^\pm(s) + c_d^{2n+1}S_B^\pm(d) + c_f^{2n+1}S_F^\pm(f) \quad (18)$$

$$S_{BF,n}^0 = c_s^{2n}S_B^0(s) + c_d^{2n}S_B^0(d) + c_f^{2n}S_F^0(f) \quad (19)$$

Where  $c_s$ ,  $c_d$  and  $c_f$  are real parameters and  $n$  can be  $0, \pm 1, \pm 2, \dots$ . These generators satisfy the commutation relations

$$[S_{BF,m}^0, S_{BF,n}^\pm] = \pm S_{BF,m+n}^\pm, \quad [S_{BF,m}^+, S_{BF,n}^-] = -2S_{BF,m+n+1}^0 \quad (20)$$

Then,  $S_{BF,m}^\mu, \mu = 0, +, -; m = \pm 1, \pm 2, \dots$  generate an affine generalized quasispin algebra  $\widehat{GQA}$  without central extension. For evaluating the eigenvalues, the eigenstates are considered as

$$|k; \nu_s \nu_n \Delta LM\rangle = NS_{BF}^+(x_1)S_{BF}^+(x_2)S_{BF}^+(x_3)\dots S_{BF}^+(x_k)|lw\rangle^{BF} \quad (21)$$

$$S_{x_i}^+ = \frac{c_s}{1 - c_s^2 x_i} S_B^+(s) + \frac{c_d}{1 - c_d^2 x_i} S_B^+(d) + \frac{c_f}{1 - c_f^2 x_i} S_F^+(f) \quad (22)$$

The lowest weight state,  $|lw\rangle^{BF}$ , is defined as

$$|lw\rangle^{BF} = |N = N_B + N_F, k_d = \frac{1}{2}(\nu_d + \frac{5}{2}), \mu_d = \frac{1}{2}(n_d + \frac{5}{2}), k_s = \frac{1}{2}(\nu_s + \frac{1}{2}), \mu_s = \frac{1}{2}(n_s + \frac{1}{2}), k_f = \frac{1}{2}(\nu_f - \frac{2j+1}{2}), \mu_f = \frac{1}{2}(n_f - \frac{2j+1}{2}), J, M\rangle \quad (23)$$

$$S_n^0|lw\rangle^{BF} = \Lambda_n^0|lw\rangle^{BF}, \quad \Lambda_n^0 = c_s^{2n}(\nu_s + \frac{1}{2})\frac{1}{2} + c_d^{2n}(\nu_d + \frac{5}{2})\frac{1}{2} + c_f^{2n}(\nu_f - \frac{2j+1}{2})\frac{1}{2} \quad (24)$$

In order to obtaining an algebraic solution for transitional region, we have used of dual algebraic structures. Such relations have often been used to effect simplifications of the calculations for two-level and multi-level systems. These relations were obtained for both bosonic and fermionic systems[13, 14]. We have established the duality relations for mixed boson-fermion system. Because of duality relationships [12–14], It is known that in even-even nuclei the base of  $U(5) \supset SO(5)$  and  $SO(6) \supset SO(5)$  are simultaneously the basis of  $SU^d(1,1) \supset U(1)$  and  $SU^{sd}(1,1) \supset U(1)$ , respectively. By use of duality relations [12–14], the Casimir operators of  $SO(5)$  and  $SO(6)$  can also be expressed in terms of the Casimir operators of  $SU^d(1,1)$  and  $SU^{sd}(1,1)$ , respectively

$$\hat{C}_2(SU^d(1,1)) = \frac{5}{16} + \frac{1}{4}\hat{C}_2(SO^B(5)) \quad (25)$$

$$\hat{C}_2(SU^{sd}(1,1)) = \frac{3}{4} + \frac{1}{4}\hat{C}_2(SO^B(6)) \quad (26)$$

For a mixed boson-fermion system, the chain of subalgebras of unitary superalgebras  $U(6/M)$  for  $j=1/2$  and  $j=3/2$  is shown in Fig.1 and Fig.2, respectively. The two-level pairing system has two dynamical symmetries defined with respect to the generalized quasispin algebras, corresponding to either the upper or lower subalgebra chains in Eq.(27).

$$GQA_1^{sf} \otimes GQA_2^{df} \supset \left\{ \begin{array}{c} GQA_{1,2}^{sdf} \\ U_1^{sf}(1) \otimes U_2^{df}(1) \end{array} \right\} \supset U_{1,2}^{sdf} \quad (27)$$

The upper subalgebra chain is corresponding to strong-coupling dynamical symmetry limit while lower chain is weak-coupling limit. For odd-A nuclei with  $j=1/2$ , we have obtained the relation between the Casimir operators  $SO(5)$  and  $GQA^{df}$  (generalized quasispin algebra of d bosons and single fermion with  $j=1/2$ ) and the Casimir operators  $SO(6)$  and  $GQA^{sdf}$  (generalized quasispin algebra of s and d bosons and single fermion with  $j=1/2$ ) according with Eqs.[25] and [26], respectively. The correspondence between the basis vectors in this case was shown in Ref.[12]. For odd-A nuclei with  $j=3/2$ , we have obtained the relation between the Casimir operators  $Spin^{BF}(5)$  and  $GQA^{df}$  (generalized quasispin algebra of d bosons and single fermion with  $j=3/2$ ) as

If  $\tau_1 = \nu_d - \frac{1}{2}$  and  $\tau_2 = \frac{1}{2}$

$$\hat{C}_2(GQA^{df}) = \frac{1}{4}\hat{C}_2(Spin^{BF}(5)) - \frac{1}{4}(\tau_1 + \frac{3}{4}) \quad (28)$$

If  $\tau_1 = \nu_d + \frac{1}{2}$  and  $\tau_2 = \frac{1}{2}$

$$\hat{C}_2(GQA^{df}) = \frac{1}{4}\hat{C}_2(Spin^{BF}(5)) - \frac{1}{4}(3\tau_1 + \frac{7}{4}) \quad (29)$$

By use of duality relations, the correspondence between the basis vectors  $Spin^{BF}(5)$  and  $GQA^{df}$  is

$$|\mathcal{N}; [N_B = N], N_F = 1, \nu_d, (\tau_1 = \nu_d - \frac{1}{2}, \tau_2), n_\Delta JM\rangle = |\mathcal{N}; k^d = \frac{1}{2}(\nu_d + \frac{5}{2}), k^{df} = \frac{\tau_1 + 2}{2}, \mu^{df} = \frac{1}{4} + \frac{1}{2}(n_d + n_f), n_\Delta JM\rangle \quad (30)$$

$$|\mathcal{N}; [N_B = N], N_F = 1, \nu_d, (\tau_1 = \nu_d + \frac{1}{2}, \tau_2), n_\Delta JM\rangle = |\mathcal{N}; k^d = \frac{1}{2}(\nu_d + \frac{5}{2}), k^{df} = \frac{1 + \tau_1}{2}, \mu^{df} = \frac{1}{4} + \frac{1}{2}(n_d + n_f), n_\Delta JM\rangle \quad (31)$$

The Casimir operator of  $Spin^{BF}(6)$  and  $GQA^{sdf}$  (generalized quasispin algebra of d and s bosons with fermion  $j=3/2$ ) has the following correspondence If  $\sigma_1 = \sigma - \frac{1}{2}$  and  $\sigma_2 = |\sigma_3| = \frac{1}{2}$

$$\hat{C}_2(GQA^{sdf}) = \frac{1}{4}\hat{C}_2(Spin^{BF}(6)) - \frac{3}{4}(\sigma_1 + \frac{3}{4}) \quad (32)$$

If  $\sigma_1 = \sigma + \frac{1}{2}$  and  $\sigma_2 = |\sigma_3| = \frac{1}{2}$

$$\hat{C}_2(GQA^{sdf}) = \frac{1}{4}\hat{C}_2(Spin^{BF}(6)) - \frac{1}{4}(\sigma_1 + \frac{3}{2}) \quad (33)$$

By use of duality relations, the correspondence between the basis vectors  $Spin^{BF}(6)$  and  $GQA^{sdf}$  is

$$|\mathcal{N}; [N_B = N], N_F = 1, \sigma, (\sigma_1, \sigma_2, \sigma_3), (\tau_1, \tau_2), n_\Delta JM\rangle = |\mathcal{N}; k^{sdf} = \frac{1}{2}(\sigma_1 + \frac{3}{2}), \mu^{sdf} = \frac{1}{4} + \frac{1}{2}(n_s + n_d + n_f), n_\Delta JM\rangle \quad (34)$$

$$|\mathcal{N}; [N_B = N], N_F = 1, \sigma, (\sigma_1, \sigma_2, \sigma_3), (\tau_1, \tau_2), n_\Delta JM\rangle = |\mathcal{N}; k^{sdf} = \frac{1}{2}(\sigma_1 + \frac{5}{2}), \mu^{sdf} = \frac{1}{4} + \frac{1}{2}(n_s + n_d + n_f), n_\Delta JM\rangle \quad (35)$$

In this article, we investigate  $U(6/2)$  and  $U(6/4)$  supersymmetry. The detailed description of the  $U(6/2)$  and  $U(6/4)$  supersymmetry in  $U(5)$  and  $O(6)$  limits can be found in Refs. [2–4]. Here we restrict ourselves only to a brief discussion of the main ideas.

## B. $U(6/2)$ Supersymmetry Model

First we considered case that fermions occupy a single particle state with angular momentum  $j=1/2$ . Thus, the underlying graded algebra is  $U(6/2)$ [2]. In order to study the occurrence of supersymmetries, one must first identify the set of nuclei belonging to the representation  $\mathcal{N}$ . Supermultiplets here contain 3 nuclei, if  $\mathcal{N} \geq 2$ . The three nuclei are characterized by[2]

$$N_B = \mathcal{N}, N_F = 0$$

$$N_B = \mathcal{N} - 1, N_F = 1$$

$$N_B = \mathcal{N} - 2, N_F = 2$$

These nuclei are alternately even-even and odd-even nuclei and have an increasing number of unpaired fermions [2]. States with  $N_F = 0$  and  $N_F = 1$  are the lowest states of the corresponding nuclei, while states with  $N_F > 2$  are at higher energies [2]. The lattice of algebras in this model is shown in Fig.(1).

In the following we will explain how derive the even-even and odd-A Hamiltonians within the U(6/2) supersymmetry scheme. By employing the generators of  $\widehat{GQA}$  and casimir operators of subalgebras, the following Hamiltonian for transitional region between U(5)-O(6) limits is prepared

$$\hat{H} = S_{BF,0}^+ S_{BF,0}^- + \alpha S_{BF,1}^0 + \beta \hat{C}_2(O^B(5)) + \delta \hat{C}_2(O^B(3)) + \gamma \hat{C}_2(\text{spin}^{BF}(3)) \quad (36)$$

$\alpha, \beta, \delta, \gamma$  are real parameters. The eigenvalues of Hamiltonian Eq.(36) can then be expressed;

$$E^{(k)} = h^{(k)} + \alpha \Lambda_1^0 + \beta \nu_d(\nu_d + 3) + \delta L_B(L_B + 1) + \gamma J(J + 1) \quad , \quad h^{(k)} = \sum_{i=1}^k \frac{\alpha}{x_i} \quad (37)$$

$$\frac{\alpha}{x_i} = \frac{c_s^2(\nu_s + \frac{1}{2})}{1 - c_s^2 y_i} + \frac{c_d^2(\nu_d + \frac{5}{2})}{1 - c_d^2 x_i} + \frac{c_f^2(\nu_f - 1)}{1 - c_f^2 x_i} - \sum_{j \neq i} \frac{2}{x_i - x_j} \quad (38)$$

### C. U(6/4) Supersymmetry Model

The case that fermions occupy a single particle state with angular momentum  $j = 3/2$  constitute the superalgebra U(6/4). Supermultiplets here contain 5 nuclei, if  $\mathcal{N} \geq 4$ . The five nuclei are characterized by [2-4]

$$N_B = \mathcal{N}, N_F = 0$$

$$N_B = \mathcal{N} - 1, N_F = 1$$

$$N_B = \mathcal{N} - 2, N_F = 2$$

$$N_B = \mathcal{N} - 3, N_F = 3$$

$$N_B = \mathcal{N} - 4, N_F = 4$$

In order to obtain Hamiltonian within the U(6/4) supersymmetry scheme, We have considered the lattice of algebras is shown in Fig.2.

So, following Hamiltonian for transitional region between U(5)-O(6) limits is prepared

$$\hat{H} = S_{BF,0}^+ S_{BF,0}^- + \alpha S_{BF,1}^0 + \beta' \hat{C}_2(\text{Spin}^{BF}(5)) + \gamma \hat{C}_2(\text{spin}^{BF}(3)) \quad (39)$$

The eigenvalues of Hamiltonian Eq.(39) can then be expressed;

$$E^{(k)} = h^{(k)} + \alpha \Lambda_1^0 + \beta'(\tau_1(\tau_1 + 3) + \tau_2(\tau_2 + 1)) + \gamma J(J + 1) \quad , \quad h^{(k)} = \sum_{i=1}^k \frac{\alpha}{x_i} \quad (40)$$

$$\frac{\alpha}{x_i} = \frac{c_s^2(\nu_s + \frac{1}{2})}{1 - c_s^2 x_i} + \frac{c_d^2(\nu_d + \frac{5}{2})}{1 - c_d^2 x_i} + \frac{c_f^2(\nu_f - 2)}{1 - c_f^2 x_i} - \sum_{j \neq i} \frac{2}{x_i - x_j} \quad (41)$$

It can be shown that Hamiltonians Eq.(36) and Eq.(39) are equivalent to a boson Hamiltonian for the even-even nuclei if acting on the  $[N] \times [0]$  representation of  $U^B(6) \times U^F(4)$  and with boson-fermion Hamiltonian for odd-A nuclei if acting on the  $[N] \times [1]$  representation of  $U^B(6) \times U^F(4)$ . By considering the neutron and proton degree of freedom in this model, we can describe all nuclei belonging to the representation  $[\mathcal{N}]$ . In odd-A nuclei, Hamiltonians Eq.(36)

and Eq.(39) are equivalent to  $O^{BF}(6)$  Hamiltonian when  $c_s = c_d = c_f$  and with  $U^{BF}(5)$  Hamiltonian if  $c_s = 0$  and  $c_d \neq c_f \neq 0$ . So, the  $c_s \neq c_d \neq c_f \neq 0$  situation just corresponds to  $U^{BF}(5) \leftrightarrow O^{BF}(6)$  transitional region. Hamiltonians Eq.(36) and Eq.(39) in even-even nuclei is equivalent to  $O(6)$  Hamiltonian when  $c_s = c_d$  and with  $U(5)$  Hamiltonian if  $c_s = 0$  and  $c_d \neq 0$  and Hamiltonian in transitional region with  $c_s \neq c_d \neq 0$ . In our calculation, we take  $c_d (= 1)$  constant value and  $c_s$  and  $c_f$  change between 0 and  $c_d$

In order to obtain the numerical results for energy spectra ( $E^{(k)}$ ) of considered nuclei in two kinds supersymmetry approach, a set of non-linear Bethe-ansatz equations (BAE) with  $k$ - unknowns for  $k$ -pair excitations must be solved also constants of Hamiltonian with least square fitting processes to experimental data is obtained [16]. To achieve this aim, we have changed variables as

$$C_s = \frac{c_s}{c_d} \leq 1, C_f = \frac{c_f}{c_d} \leq 1, y_i = c_d^2 x_i$$

$$\frac{\alpha}{y_i} = \frac{C_s^2(\nu_s + \frac{1}{2})}{1 - C_s^2 y_i} + \frac{(\nu_d + \frac{5}{2})}{1 - y_i} + \frac{C_f^2(\nu_f - \frac{2j+1}{2})}{1 - C_f^2 y_i} - \sum_{j \neq i} \frac{2}{y_i - y_j} \quad (42)$$

The quantum number ( $k$ ) is related to  $\mathcal{N}$  by  $\mathcal{N} = 2k + \nu_s + \nu_d + \nu_f$ . The quality of the fits is quantified by the values of  $\sigma = (\frac{1}{N_{tot}} \sum_{i,tot} |E_{exp}(i) - E_{Cal}(i)|^2)^{\frac{1}{2}}$  (keV) and  $\phi = \frac{\sum_i |E_i^{theor} - E_i^{exp}|}{\sum_i E_i^{exp}}$  (%) ( $N_{tot}$  the number of energy levels where included in the fitting processes) [2–4]. A measure of the breaking of the supersymmetry scheme, the average absolute deviation divided by the average excitation energy, give with  $\phi$  parameter [2, 4]. The method for optimizing the set of parameters in the Hamiltonian ( $\beta, \gamma, \delta$ ) includes carrying out a least-square fit (LSF) of the excitation energies of selected states [16].

#### D. E2 transition probabilities

The observables such as electric quadrupole transition probabilities,  $B(E2)$ , as well as quadrupole moment ratios within the low-lying state provide important information about the nuclear structure and  $QPTs$ . In this section we discuss the calculation of E2 transition strengths for  $j=1/2$  and  $j=3/2$ . Supersymmetry implies that all transitions in nuclei belonging to the same supermultiplet be explained by the same operator[2]. The electric quadrupole transition operator  $\hat{T}^{(E2)}$  in odd-A nuclei consists of a bosonic and a fermionic part[2, 17, 18]. In the  $j = 1/2$  case, the E2 transitions for even-even and odd-A nuclei are completely determined by the bosonic part of the E2 operator[2]. The bosonic part have the specific selection rules, where for former term  $\Delta\nu_d = \pm 1$ ,  $|\Delta L| \leq 2$  and for latter  $\Delta\nu_d = 0, \pm 2$ ,  $|\Delta L| \leq 0, 4$ . In the  $j = 3/2$  case, we also consider the portion of fermionic term[2, 17, 18].

$$\hat{T}^{(E2)} = \hat{T}_B^{(E2)} + \hat{T}_F^{(E2)} \quad (43)$$

With

$$T_{B,\mu}^{(E2)} = q_2 [s^+ \times \tilde{d} + d^+ \times \tilde{s}]_{\mu}^{(2)} + q_2' [d^+ \times \tilde{d}]_{\mu}^{(2)} = q_B Q_{B,\mu} \quad (44)$$

$$Q_{B,\mu} = [s^+ \times \tilde{d} + d^+ \times \tilde{s}]_{\mu}^{(2)} + \chi [d^+ \times \tilde{d}]_{\mu}^{(2)} \quad (45)$$

$$T_F^{(E2)} = q_f \sum_{jj'} Q_{jj'} [a_j^+ \times \tilde{a}_{j'}]^{(2)} \quad (46)$$

Where  $Q_B$  and  $Q_{jj'}$  are the boson and fermion quadrupole operator and  $q_B$  and  $q_f$  are the effective boson and fermion charges[2, 17, 18].

The reduced electric quadrupole transition rate between the  $J_i \rightarrow J_f$  states is given by [1, 2]

$$B(E2; \alpha_i J_i \rightarrow \alpha_f J_f) = \frac{|\langle \alpha_f J_f || T^{(E2)} || \alpha_i J_i \rangle|^2}{2J_i + 1} \quad (47)$$

For evaluating  $B(E2)$ , we have calculated the matrix elements of  $T(E2)$  operators between the eigenstates of Eq.(21) that the normalization factor obtain as:

$$N = \sqrt{\frac{1}{\prod_{p=1}^k \sum_{i=p}^k \left( \frac{2C_s^2(k-p+\frac{1}{2})(\nu_s+\frac{1}{2})}{(1-C_s^2 y_{k+1-p})(1-C_s^2 y_i)} + \frac{2(k-p+\frac{1}{2})(\nu_d+\frac{5}{2})}{(1-y_{k+1-p})(1-y_i)} - \frac{2C_f^2(k-p+\frac{1}{2})(\nu_f-\frac{2j+1}{2})}{(1-C_f^2 y_{k+1-p})(1-C_f^2 y_i)} \right)}}} \quad (48)$$

We calculate fermion part for  $j=3/2$  by using Eq.(49)[17, 18]

$$\langle \nu_B, \nu_F, (\tau_1, \tau_2), L_{BF}, J || T_F^{(\lambda, \mu)} || \nu'_B, \nu'_F, (\tau'_1, \tau'_2), L'_{BF}, J' \rangle = \sum_{\nu, L} \sum_{\nu', L'} \xi_{N+1/2, \tau_1, J}^{N, \nu, L} \xi_{N+1/2, \tau'_1, J'}^{N, \nu', L'} (-1)^{L+J'+3/2} (-1)^{J-J'} \left\{ \begin{matrix} 3/2 & J & L \\ J' & 3/2 & 2 \end{matrix} \right\} \langle 3/2 || T_F^{(E2)} || 3/2 \rangle \quad (49)$$

Where  $\xi$  is isoscalar factor and  $\langle 3/2 || T_F^{(E2)} || 3/2 \rangle$  is a single-particle matrix element that is obtained as[2, 17, 18]

$$\langle j || (a_{j_1}^\dagger \times \tilde{a}_{j_2})^{(\lambda)} || j' \rangle = -\sqrt{2\lambda + 1} \delta_{j_2, j'} \delta_{j_1, j} \quad (50)$$

A test of supersymmetry is to see the extent to which the electric quadrupole transition probabilities of even-even and odd-A nuclei can be describe with the same coefficients of Eq.(47). To determine boson effective charge, we have extracted these quantities from the empirical B(E2) values via least square technique. In the fitting process, empirical transition rates of both of even-even and odd-A nuclei were used.

### III. QUANTAL ANALYSIS

This section presented the calculated phase transition observables such as level crossing, expectation values of the d-boson and the fermion number operators.

#### A. energy spectrum and level crossing

In order to display how the energy levels change within the whole range of the  $C_s$  and  $C_f$  control parameters, the energy surfaces  $E(C_s, C_f)$  with the other parameters fixed can be defined and calculated using procedure that explained in sec.(II). Fig.3 and Fig.4 show the energy surfaces of Hamiltonian of Eq.(36) and Eq.(39) for the neighboring even-even (left panel) and odd-A nuclei (right panel) with  $N = 10$ , respectively. The calculation are performed by considering the same fit parameters for neighboring even-even and odd-A nuclei, where in Fig.3 the fixed parameters are  $\alpha = 1000\text{keV}$ ,  $\beta = 3.14\text{keV}$ ,  $\delta = -5.26\text{keV}$ ,  $\gamma = 0.0439\text{keV}$  and Fig.4 obtained with  $\alpha = 1000\text{keV}$ ,  $\beta' = -1.29\text{keV}$ ,  $\gamma = 6.05\text{keV}$ . Figs show how the energy levels evolve from one phase to the other as a function of  $C_s$  and  $C_f$  control parameters. These Figures clearly show how the transition from one dynamical symmetry to another occurs. It can be seen from Figs that numerous level crossings occur. The crossings are due to the fact that  $\nu_d$ , O(5) quantum number called seniority, is preserved along the whole path between O(6) and U(5)[19, 20].

#### B. expectation values of the d-boson number operator

An appropriate quantal order parameter is:

$$\langle \hat{n}_d \rangle = \frac{\langle \psi | \hat{n}_d | \psi \rangle}{N}$$

In order to obtain  $\langle \hat{n}_d \rangle$ , we act  $s_m^0$  on the eigenstate,  $|k; \nu_s \nu n_\Delta LM\rangle$

$$\langle \hat{n}_d \rangle = \frac{2C_s^2 C_f^2 (\Lambda_0^0 + k) - 2(C_s^2 + C_f^2) (\Lambda_1^0 + ky_1^{-1}) + 2(\Lambda_2^0 + ky_2^{-2})}{N(1 - C_s^2)(1 - C_f^2)} - \frac{5}{2N} \quad (51)$$

Fig.5 and Fig.6 show the expectation values of the d-boson number operator for the lowest states even-even (left panel) and odd-A nuclei (right panel) as a function of control parameters for  $j=1/2$  and  $j=3/2$  with  $N=10$  bosons, respectively. Fig.5 and Fig.6 (left panel) display that the expectation values of the number of d bosons for each L,  $n_d$ , remain approximately constant for  $C_s < 0.45$  and only begin to change rapidly for  $C_s > 0.45$ . The near constancy of  $n_d$  for  $C_s < 0.45$ , is a obvious indication that U(5) dynamical symmetry preserves in this region to a high degree and also the  $n_d$  values change rapidly with  $C_s$  over the range  $0.65 \leq C_s \leq 1$ .



### C. expectation values of the fermion number operator

The expectation values of the fermion number operator are obtained as

$$\langle \hat{n}_f \rangle = \frac{\langle \psi | \hat{n}_f | \psi \rangle}{N} = \frac{2(1 + C_s^2)(\Lambda_0^0 - \Lambda_1^0 + k(1 - y_1^{-1})) - 2(\Lambda_0^0 - \Lambda_2^0 + k(1 - y_2^{-2}))}{N(1 - C_f^2)(C_s^2 - C_f^2)} + \frac{2j + 1}{2N} \quad (52)$$

Fig.7 and Fig.8 show also  $\langle n_f \rangle$  as a function of the  $C_s$  and  $C_f$  control parameters.

It can be seen from figs that combination of multi-symmetry in the point of phase transition cause dissimilar behavior with neighboring points that representing the transition of u(5) limit to O(6) limit.

## IV. EXPERIMENTAL EVIDENCE

This section presented the calculated results of low-lying states of Rh-Ru Supermultiplets and Zn - Cu Supermultiplets. The results include energy levels and the B(E2) values and Key observables of E(5) and E(5/2j+1) symmetry.

### A. The Rh-Ru Supermultiplets

Nuclei in the mass region around  $A \sim 100$  have transitional characteristics intermediate between spherical and gamma-unstable shapes [21, 22]. Stachel et al.[23] have been studied the Ru isotopes and are found that these isotopes have U(5)-O(6) transition features. The odd-A Rh isotopes were studied in the framework IBFM by Vervier and Janssens [24] and Refs.[16, 21, 22, 25]. A. Frank and collaborators have studied the Rh-Ru Supermultiplets by using supersymmetry approach [6]. They have studied successfully a combination of  $U^{BF}(5)$  and  $SO^{BF}(6)$  symmetry by using U(6/12) supersymmetry for the Ru and Rh isotopes. We have also analyzed the negative parity states of the odd-proton nuclei,  ${}_{45}^{101-109}\text{Rh}$  and positive parity states of the even-even nuclei,  ${}_{44}^{100-108}\text{Ru}$ . The negative parity states in the odd-even nuclei Rh are built mainly on the  $2p_{\frac{1}{2}}$  shell model orbit[21]. In order to obtain energy spectrum and realistic calculation for these nuclei, we need to specify Hamiltonian parameters Eq.(36). According to the supersymmetry between bosons and fermions, the fermion is transformed into a boson, the system is described by the same set of parameters thus to achieve a better fit, states of both of even-even and odd-A nuclei were used. Eigenvalues of these systems are obtained by solving Bethe-Ansatz equations with least square fitting processes to experimental data to obtain constants of Hamiltonian. The best fits for Hamiltonian's parameters, namely  $\alpha$ ,  $\beta$ ,  $\delta$  and  $\gamma$ , used in the present work are shown in table 1. Fig.9 and Fig.10 show a comparison between the available experimental levels and the predictions of our results for the  ${}_{45}^{101-109}\text{Rh}$  and  ${}_{44}^{100-108}\text{Ru}$  isotopes in the low-lying region of spectra. The quantum numbers of different states of each isotope and a comparison between theoretical prediction and experimental values for considered isotopes are presented in Tables.2(a,b...e). An acceptable degree of agreement is obvious between them.

The most important successful nuclear model characteristic is a good description of electromagnetic properties of the nucleus in addition to its energy spectrum. So, we have calculated B(E2) transition rates for Ru-Rh Supermultiplets. In the fitting process, because there is no empirical data for Rh isotopes except  ${}^{103}\text{Rh}$  we have used only of the even-mass Ru experimental data for extracting of effective charge parameters. In  ${}^{102}\text{Ru} - {}^{103}\text{Rh}$  supermultiplet, we have used of experimental transition rates of both nuclei. Extracted values for effective charge parameters have presented in Table 3. Tables.4(a,b,c,d) show experimental and calculated values of B(E2) for negative parity states of Rh and positive parity states of Ru.

### B. The Zn-Cu Supermultiplets

In order to test the predictions of the U(6/4) scheme in dynamical symmetry limits and transition region, we choose the negative parity states of the odd-proton nuclei,  ${}^{61-69}\text{Cu}$  and positive parity states of the even-even nuclei,  ${}^{62-70}\text{Zn}$ . These nuclei have not considered in other theoretical studies completely but for some of them which we have found similar counterparts. The Cu isotopes across the N=40 shell closure and have a single proton outside the Z=28 closed shell. The ground state spin/parity of the odd-A copper isotopes( Between  ${}^{57}\text{Cu}$  and  ${}^{69}\text{Cu}$ ) is  $(\frac{3}{2})^-$ . The low-lying levels of  ${}^{63,65}\text{Cu}$  were studied by Bijker and Kota in 1984 [37]. They showed that the Spin(5) symmetry could occur in the odd-proton nuclei in the Cu region with the odd-proton occupying the  $2p_{3/2}$  orbit. Since the low-lying negative parity states in  ${}^{63,65}\text{Cu}$  are built mainly on the  $2p_{3/2}$  shell model orbit and the adjacent even-even nuclei  ${}^{64,66}\text{Zn}$  show

a vibrational type of spectrum, it has been suggested [37, 38], that the Cu-Zn mass-region provides experimental evidence for the existence of the Spin(5) spinor symmetry and the U(6/4) supersymmetry [37]. The odd-even nuclei  $^{63,65}\text{Cu}$  alone provide a test of the Spin(5) symmetry, while the pairs of nuclei Zn-Cu provide a test of the U(6/4) supersymmetry [37]. Since vibrational nuclei are known to exhibit other excitation modes such as quasi particle modes or intruder states due to the excitation of two protons into the next major shell in Zn [39], great care must be taken in comparing with experiment. We have used a similar procedure as has done for Ru-Rh supermultiplets calculations to extract the parameters of Hamiltonian Eq.(39) for Zn-Cu supermultiplets. In the fitting process, in addition to the states in Cu, the states of Zn isotopes were considered. The best fits for Hamiltonian's parameters, namely  $\alpha$ ,  $\beta'$  and  $\gamma$ , used in the present work are shown in table 5. Figs.11 and 12 show the comparison of the experimental and the theoretical level scheme. Experimental data of  $^{61-69}\text{Cu}$  and  $^{62-70}\text{Zn}$  isotopes was taken from Refs.[40-49]. The quantum numbers of different states of each isotope and a comparison between theoretical prediction and experimental values for considered isotopes are presented in Tables.6(a,b,...,e).

we have also calculated B(E2) transition rates for Zn-Cu Supermultiplets. To determine boson effective charge, we have extracted these quantities from the empirical B(E2) values via least square technique. In the fitting process, we have used of experimental transition rates of both nuclei in a Supermultiplet. Extracted values for effective charge parameters have presented in Tables 7. Tables.8(a,b,..,e) show experimental and calculated values of B(E2) for negative parity states of Cu and positive parity states of Zn. In Zn-Cu Supermultiplet, improved results may be obtained by considering neutron and proton degree of freedom separately.

In the following, we concentrated upon those distinguishing observables which vary along the U(5)- SO(6) transition. The observables such as the energy ratios, the B(E2) values that are most sensitive to the U(5)-O(6) structural transition. M.A.Caprio and F.Iachello [18] obtained analytic descriptions for transitional nuclei near the critical point. The solutions provided baselines for experimental studies of even- even [E(5)] and odd-mass E(5/4) nuclei near the critical point of the spherical to gamma-unstable phase transition. Their results have provided benchmarks for nuclei near the critical point of the U(5)-O(6) phase transition and can be used as a basis for comparison with experiment. So, we have also calculated these quantities for the Ru-Rh and Zn-Cu supermultiplets by using their method and performed an analysis for these isotopes. One of the most basic structural predictions of U(5) – O(6) transition is a  $R_{\frac{3}{2}} = \frac{E(4_1^+)}{E(2_1^+)}$  value. The ratio equal to 2.2-2.3 indicates the spectrum of transitional nuclei [18, 50, 51]. Thus, we calculated this quantity for even-even Ru and Zn Isotopes. Fig.13(a) and Fig.14(a) show  $R_{\frac{3}{2}}$  prediction along with the experimental values for Ru and Zn isotopes, respectively. We have also calculated observables such as  $\frac{E(0_2^+)}{E(2_1^+)}$ , the vibrational excitation measure, values for control parameter, namely the ratio of shape phase transition, and ratios  $B(\frac{E2;4_1^+ \rightarrow 2_1^+}{E2;2_1^+ \rightarrow 0_1^+})$  and  $B(\frac{E2;0_2^+ \rightarrow 2_1^+}{E2;2_1^+ \rightarrow 0_1^+})$ . The comparison with experiment for these quantities in Ru and Zn isotopes is summarized in Table.9 and Table.10, respectively.

Because of the occurrence of single particle orbitals that can considerably perturb the spectrum and electromagnetic transition strengths, comparison of the critical point description with experimental data in odd-mass nuclei is more difficult than even-even nuclei[18]. For Cu and Rh isotopes, we calculated only the energy ratio quantity. Fig.13(b) and Fig.14(b) show  $\frac{E(\nu_d=2)}{E(\nu_d=1)}$  prediction along with the experimental values for these isotopes.

From these figures and tables, one can conclude, the calculated energy spectra in this approach are approximately in good agreements with the experimental data. It means that our suggestion to use this transitional Hamiltonian for the description of the Rh-Ru and Zn-Cu supermultiplets would not have any contradiction with other theoretical studies done with special hypotheses about mixing of intruder and normal configurations. On the other hand, predictions of our model for the control parameters of considered supermultiplet,  $C_s$  and  $C_f$ , describe the vibrational, i.e.  $C_s = 0$ , or rotational, namely  $C_s = 1$ , and also  $C_f \neq 0$  for odd-A nuclei and  $C_f = 0$  for even-even nuclei, confirm this mixing of both vibrating and rotating structures in these nuclei when  $C_s \sim 0.5 \rightarrow 0.65$ . The values of the control parameter,  $C_s$ , suggest structural changes in nuclear deformation and shape-phase transitions in Rh-Ru and Zn-Cu supermultiplets. we proposed  $C_s \sim 0.5 \rightarrow 0.65$  as critical point. We conclude from the values of control parameter which has been obtained, observables such as the energy ratios and the B(E2) values that  $^{104}\text{Ru} - ^{105}\text{Rh}$  and  $^{64}\text{Zn} - ^{63}\text{Cu}$  supermultiplets are as the best candidates for U(5) – O(6) transition. Also, theoretical B(E2)transition probabilities of the Rh-Ru and Zn-Cu supermultiplets, which have obtained by using the model perspectives, exhibit nice agreement with experimental ones.

### C. two-neutron separation energies

Shape phase transitions in nuclei can be studied experimentally by considering the behavior of the ground state energies of a series of isotopes, or, more conveniently, the behavior of the two-neutron separation energies,  $S_{2n}$  [1, 52]. On the other hand, the ground-state two-neutron separation energies,  $S_{2n}$ , are observables very sensitive to the details

of the nuclear structure and indirect test of the supersymmetry scheme. The occurrence of continuities in the behavior of two-neutron separation energies describe a second-order shape-phase transition between spherical and  $\gamma$  - unstable rotor limits [1, 52]. In due to, we have investigated the evolution of two-neutron separation energies along the Ru, Rh, Zn and Cu isotopic chains by both experimental and theoretical values, which have been presented in Fig.15 and Fig.16.

Two-neutron separation energies for even-even and odd-even nuclei defined by [2, 4]

$$S_2(\mathcal{N}, N_f = 0) = E_B(\mathcal{N} + 1, N_f = 0) - E_B(\mathcal{N}, N_f = 0) \quad (53)$$

$$S_2(\mathcal{N}, N_f = 1) = E_B(\mathcal{N} + 1, N_f = 1) - E_B(\mathcal{N}, N_f = 1) \quad (54)$$

Where  $E_B$  denotes the binding energy. It can be shown that if supersymmetry applies, the separation energies in even-even and odd-even nuclei should be linear functions of  $\mathcal{N}$  as [2, 4]

$$S_2(\mathcal{N}, N_f = 0) = S_2(\mathcal{N}, N_f = 1) = D_1 + C_1\mathcal{N} \quad (55)$$

Using the  $S_{2n}$  empirical values for these isotopic chains [36] we have extracted  $D_1 = 2.28 \times 10^4, 3.0814 \times 10^4$  MeV and  $C_1 = -898.5, -2.5 \times 10^3$  MeV for Ru-Rh and Zn-Cu supermultiplets, respectively. Then, we obtained the two-neutron separation energies, which are shown in Fig.15 and Fig.16, together with the experimental values.

It can be seen from Fig.15 and Fig.16 that exist continuities (linear variation) in the behavior of two-neutron separation energies thus the phase transition for Ru, Rh, Zn and Cu isotopic chains is of second order and also approximately equal slopes for Ru(Zn) even-even and Rh(Cu) odd-mass nuclei is a result of supersymmetry scheme. Our result Confirmed the predictions of done in refs. [1,2,4,52].

## V. CONCLUSIONS

In this paper, we have proposed exactly-solvable supersymmetry Richardson-Gaudin (R-G) model for transitional region. We apply supersymmetry ideas to the description of even and odd nuclei and display that several states in many nuclei can be explained by schemes based on the  $U(6/2)$  and  $U(6/4)$  supergroups. We have employed the nuclear supersymmetry approach for description of the transitional region between spherical and gamma -unstable phase shape in addition to dynamical symmetry limits in one chain isotopic. Key observables of phase transition such as level crossing, expectation values of the d-boson and fermion number operator were calculated. New experimental data on the even-mass ruthenium and the odd-mass rhodium isotopes and Zn-Cu Supermultiplets were used to test the predictions of the new Supersymmetry scheme in dynamical symmetry limits and transition region and performed an analysis for these isotopes via a GQA-based Hamiltonian. The results indicate that the energy spectra of the Rh-Ru and Zn-Cu Supermultiplets can be reproduced approximately well. The observables such as the energy ratios, the  $B(E2)$  values that are most sensitive to the  $U(5)$ - $O(6)$  structural transition were calculated and compared with the available experimental data. Our results show that the Rh-Ru and Zn-Cu Supermultiplets have gamma-unstable rotor features but the vibrational character is dominant and also  $^{104}Ru - ^{105}Rh$  and  $^{64}Zn - ^{63}Cu$  Supermultiplets are as the best candidates for  $U(5) - O(6)$  transition.

- 
- [1] F. Iachello and A. Arima, *The interacting boson model* (Cambridge University Press, 1987).
  - [2] F. Iachello and P. Van Isacker, *The interacting boson-fermion model* (Cambridge University Press, 1991).
  - [3] F. Iachello, *Phys. Rev. Lett.* 44, 772 (1980).
  - [4] A. B. Balantekin, I. Bars, and F. Iachello, *Phys. Rev. Lett.* 47, 19 (1981); *Nucl. Phys. A* 370, 284 (1981).
  - [5] A. Metz et al., *Phys. Rev. Lett.* 83, 1542 (1999); *Phys. Rev. C* 61, 064313 (2000); J. Groger et al., *Phys. Rev. C* 62, 064304 (2000).
  - [6] A. Frank, P. Van Isacker and D.D. Warner, *Phys. Lett. B* 197, 474 (1987).
  - [7] P. VAN Isacker, A. Frank and Hong-Zhou Sun, *ANNALS OF PHYSICS* 157, 183-231 (1984).
  - [8] F. Iachello, N. V. Zamfir, and R. F. Casten, *Phys. Rev. Lett.* 81, 1191 (1998).
  - [9] R. F. Casten, D. Kusnezov, and N. V. Zamfir, *Phys. Rev. Lett.* 82, 5000 (1999).
  - [10] F. Iachello, *Physical review letters* 95, 052503 (2005).
  - [11] J.Jolie, S. Heinze, P. Van Isacker, and R.F.Casten, *Phys. Rev. C* 70, 011305(R)(2004).
  - [12] F. Pan and J. Draayer, *Nuclear Physics A* 636, 156 (1998).
  - [13] M. Caprio, J. Skrabacz, and F. Iachello, *Journal of Physics A: Mathematical and Theoretical* 44, 075303 (2011).
  - [14] D. Rowe, M. Carvalho, and J. Repka, *Reviews of Modern Physics* 84, 711 (2012).
  - [15] P.D.Jarvis, Mei Yang and B.G.Wybourne, *Journal of Mathematical Physics* 28,1192 (1987).
  - [16] M. A. Jafarizadeh, M. Ghapanvari, and N. Fouladi,*Phys. Rev. C* 92, 054306 (2015).
  - [17] C.E. Alonso, J.M. Arias, A. Vitturi, *Phys. Rev. C* 75 064316(2007).
  - [18] M. Caprio and F. Iachello, *Nuclear Physics A* 781, 26 (2007).
  - [19] P. Cejnar, S. Heinze, and J. Jolie, *Phys. Rev. C* 68, 034326(2003).
  - [20] J.Jolie, S. Heinze, P. Van Isacker, and R.F.Casten, *Phys.Rev. C* 70, 011305(R)(2004).
  - [21] J. Arias, C. Alonso, and M. Lozano, *Nucl. Phys. A* 466, 295 (1987).
  - [22] G. Maino, A. Ventura, A. Bizzeti-Sona, and P. Blasi,*Z. Phys. A* 340, 241(1991).
  - [23] J. Stachel, P. Van Isacker and K. Heyde, *Phys. Rev. C* 25 (1982) 650
  - [24] J. Vervier and R.V.F. Janssens, *Phys. Lett.B* 108 (1982) 1.
  - [25] P. Van Isacker, J. Jolie, K. Heyde, M. Waroquier, J. Moreau and O. Scholten, *Phys. Lett. B* 149 (1984) 26.
  - [26] Balraj Singh, *Nuclear Data Sheets* 109 (2008) 297-516.
  - [27] Jean Blachot, *Nuclear Data Sheets* 45, 701 (1985) .
  - [28] D.De Frenne, *Nuclear Data Sheets* 110 (2009) 1745-1915.
  - [29] D.De Frenne, *Nuclear Data Sheets* 110 (2009) 2081-2256.
  - [30] Jean Blachot, *Nuclear Data Sheets* 108 (2007) 2035-2172.
  - [31] D. De Frenne and E. Jacobs, *Nuclear Data Sheets* 105 (2005) 775-958.
  - [32] D.De Frenne and A. Negret, *Nuclear Data Sheets* 109 (2008) 943-1102.
  - [33] Jean Blachot, *Nuclear Data Sheets* 109 (2008) 1383-1526.
  - [34] Jean Blachot, *Nuclear Data Sheets* 90, 135 (2000).
  - [35] Jean Blachot, *Nuclear Data Sheets* 107 (2006) 355-506.
  - [36] National nuclear data center, <http://www.nndc.bnl.gov/chart/reColor.jspnewColor=dm>.
  - [37] R. Bijker and V. K. B. Kota, *Ann. Phys. (N.Y.)* 156, 110(1984).
  - [38] J.Vervier, private communication, to be published.
  - [39] C. H. Druce, I. D. McCullen, P. D. Duval, and B. R. Barrett, *J. Phys. G:* 8 (1982), 1565.
  - [40] Kazimierz Zuber and Balraj Singh, *Nuclear Data Sheets* 125 (2015) 1-200.
  - [41] Alan L. Nichols, Balraj Singh and Jagdish K. Tuli, *Nuclear Data Sheets* 113 (2012) 973-1114.
  - [42] Bai Erjun and Huo Junde, *Nuclear Data Sheets* 92, 147 (2001).
  - [43] Balraj Singh, *Nuclear Data Sheets* 108 (2007) 197-364.
  - [44] E. Browne and J. K. Tuli, *Nuclear Data Sheets* 111 (2010) 2425-2553.
  - [45] E. Browne and J. K. Tuli, *Nuclear Data Sheets* 111 (2010) 1093-1209.
  - [46] Huo Junde, Huang Xiaolong and J.K. Tuli, *Nuclear Data Sheets* 106 (2005) 159-250.
  - [47] E.A. McCutchan, *Nuclear Data Sheets* 113 (2012) 1735-1870.
  - [48] C.D. Nesaraja, *Nuclear Data Sheets* 115 (2014) 1-134.
  - [49] J. K. Tuli, *Nuclear Data Sheets* 103 (2004) 389-514.
  - [50] R. F. Casten and N. V. Zamfir, *Phys. Rev. Lett.* 85,3584 (2000).
  - [51] R. Casten and E. McCutchan, *Journal of Physics G: Nuclear and Particle Physics* 34, R285 (2007).
  - [52] N. V. Zamfir, S. Anghel, and G. Cata-Danil, *AIP Conf. Proc.No.* 1072, 118 (AIP, New York, 2008).

Table 1.Parameters of Hamiltonian Eq.(36) used in the calculation of the Ru-Rh Supermultiplets. All parameters are given in keV.

Nucleus	$\mathcal{N}$	$C_s$	$C_f$	$\alpha$	$\beta$	$\delta$	$\gamma$	$\sigma$	$\phi$
$^{100}\text{Ru} - ^{101}\text{Rh}$	6	0.38	0.99	279.2	3.974	7.89	-2.217	164.53	11.23%
$^{102}\text{Ru} - ^{103}\text{Rh}$	7	0.23	0.8	170.32	0.8854	-1.207	6.874	104.74	6.38 %
$^{104}\text{Ru} - ^{105}\text{Rh}$	8	0.54	0.99	70.61	0.1915	46.69	-15.123	137.8	13.2%
$^{106}\text{Ru} - ^{107}\text{Rh}$	9	0.34	0.7	197.52	0.329	51.14	-35.72	128.73	11.79 %
$^{108}\text{Ru} - ^{109}\text{Rh}$	10	0.58	0.99	248.2	4.464	1.21	-7.863	128.54	12.8 %

Table 2a.Energy spectra for  $^{100}_{44}\text{Ru} - ^{101}_{45}\text{Rh}$  isotope.The experimental data for  $^{100}_{44}\text{Ru} - ^{101}_{45}\text{Rh}$  supermultiplet are taken from [26, 27, 36].

Nuclei	$J^\pi$	$K$	$\nu_d$	$E_{exp}(\text{keV})$	$E_{cal}(\text{keV})$	
$^{100}_{44}\text{Ru}$	$0_1^+$	3	0	0	0	
	$2_1^+$	2	1	539.5	503	
	$0_2^+$	3	2	1130.3	1284.9	
	$2_2^+$	2	2	1362.16	1219.1	
	$4_1^+$	2	2	1226.48	1126.72	
	$0_3^+$	1	3	1740.98	1938.6	
	$3_1^+$	1	3	1881.04	2018.3	
	$2_3^+$	2	1	1865.1	2018.3	
	$4_2^+$	1	3	2062.51	2086.5	
	$6_1^+$	1	3	2076.1	2256.9	
	$0_4^+$	3	0	2051.65	2290.8	
	$2_4^+$	2	2	2099.1	2207.7	
	$^{101}_{45}\text{Rh}$	$(1/2)_1^-$	2	0	0	0
		$(3/2)_1^-$	2	1	305.5	315.4
$(5/2)_1^-$		2	1	305.5	292.3	
$(3/2)_2^-$		1	2	355.3	536.9	
$(5/2)_2^-$		1	2	355.3	425	
$(7/2)_1^-$		1	2	851.4	860.4	
$(9/2)_1^-$		1	2	851.4	826.7	
$(9/2)_2^-$		1	2	899.3	1104.2	
$(5/2)_3^-$		2	1	996.4	914.4	
$(3/2)_4^-$		1	2	1058	895.7	

Table 2b. Energy spectra for  $^{102}_{44}Ru - ^{103}_{45}Rh$  isotope. The experimental data for  $^{102}_{44}Ru - ^{103}_{45}Rh$  supermultiplet are taken from [28, 29, 36].

Nuclei	$J^\pi$	$K$	$\nu_d$	$E_{exp}(\text{keV})$	$E_{cal}(\text{keV})$	
$^{102}_{44}Ru$	$0^+_1$	3	0	0	0	
	$2^+_1$	3	1	475.08	510.8	
	$0^+_2$	3	0	943.69	828.9	
	$2^+_2$	2	2	1103.15	1267.4	
	$4^+_1$	2	2	1106.36	1215	
	$0^+_3$	2	3	1837.10	1702.6	
	$3^+_1$	2	3	1521.67	1621.4	
	$2^+_3$	3	1	1580.56	1577.1	
	$4^+_2$	2	3	1602.9	1671.4	
	$6^+_1$	2	3	1873.23	1809	
	$0^+_4$	3	0	1968.66	2131	
	$2^+_4$	2	2	2036.9	2360.3	
	$^{103}_{45}Rh$	$(1/2)^-_1$	3	0	0	0
		$(3/2)^-_1$	2	1	294.984	276.8
		$(5/2)^-_1$	2	1	357.408	325.5
		$(1/2)^-_2$	3	0	803.07	966.5
$(3/2)^-_2$		2	2	803.07	647.1	
$(7/2)^-_1$		2	2	847.58	717.6	
$(5/2)^-_2$		2	2	880.47	689.9	
$(9/2)^-_1$		2	2	920.1	794.5	
$(3/2)^-_3$		2	2	1277.04	1247.9	
$(13/2)^-_1$		2	3	1637.64	1551.1	
$(15/2)^-_1$		1	4	2221.2	2255.5	
$(17/2)^-_1$		1	4	2345.35	2400.9	

Table 2c. Energy spectra for  $^{104}_{44}Ru - ^{105}_{45}Rh$  isotope. The experimental data for  $^{104}_{44}Ru - ^{105}_{45}Rh$  supermultiplet are taken from [30, 31, 36].

Nuclei	$J^\pi$	$K$	$\nu_d$	$E_{exp}(\text{keV})$	$E_{cal}(\text{keV})$	
$^{104}_{44}Ru$	$0^+_1$	4	0	0	0	
	$2^+_1$	3	1	358.02	406.3	
	$0^+_2$	4	0	988.3	1294.3	
	$2^+_2$	3	2	893.1	1139.4	
	$4^+_1$	3	2	888.5	944.9	
	$3^+_1$	2	3	1242.4	1233.5	
	$2^+_3$	3	1	2285	2103.8	
	$^{105}_{45}Rh$	$(1/2)^-_1$	3	0	129.781	175.9
		$(3/2)^-_1$	3	1	392.65	447.4
		$(5/2)^-_1$	3	1	455.61	371.8
$(3/2)^-_2$		2	2	762.11	642.9	
$(3/2)^-_3$		2	1	783	642.9	
$(5/2)^-_2$		2	2	817	1006.7	
$(7/2)^-_1$		2	2	817	900.8	
$(5/2)^-_3$		2	3	866	1112.6	
$(7/2)^-_2$		2	3	898	1115.1	
$(7/2)^-_3$		2	2	976	1009.2	
$(9/2)^-_1$		2	2	976	802.5	
$(3/2)^-_4$		2	3	1147	1174.2	
$(5/2)^-_4$		3	1	1147	987.7	

Table 2d. Energy spectra for  $^{106}_{44}Ru - ^{107}_{45}Rh$  isotope. The experimental data for  $^{106}_{44}Ru - ^{107}_{45}Rh$  supermultiplet are taken from [32, 33, 36].

Nuclei	$J^\pi$	$K$	$\nu_d$	$E_{exp}(\text{keV})$	$E_{cal}(\text{keV})$
$^{106}_{44}Ru$	$0^+_1$	4	0	0	0
	$2^+_1$	4	1	270.07	321.1
	$0^+_2$	4	0	990.62	1086.5
	$2^+_2$	3	2	792.31	613.1
	$4^+_1$	3	2	714.69	811.3
	$3^+_1$	3	3	1091.55	974
	$2^+_3$	4	1	1392.21	1173.6
	$4^+_2$	3	3	2367	2321
	$6^+_1$	3	3	1295.8	1232.6
	$^{107}_{45}Rh$	$(1/2)^-_1$	4	0	268.36
$(3/2)^-_1$		3	1	485.66	613.4
$(5/2)^-_1$		3	1	543.84	451.3
$(9/2)^-_1$		3	2	559.97	662.7
$(3/2)^-_2$		3	2	752.55	711.7
$(5/2)^-_2$		3	2	877.75	1139.8
$(3/2)^-_3$		3	2	974.44	1146.5
$(5/2)^-_3$		2	3	974.44	967.9
$(7/2)^-_1$		3	2	974.44	994.3
$(3/2)^-_4$		2	3	1009.76	1146.5

Table 2e. Energy spectra for  $^{108}_{44}Ru - ^{109}_{45}Rh$  isotope. The experimental data for  $^{108}_{44}Ru - ^{109}_{45}Rh$  supermultiplet are taken from [34-36].

Nuclei	$J^\pi$	$K$	$\nu_d$	$E_{exp}(\text{keV})$	$E_{cal}(\text{keV})$
$^{108}_{44}Ru$	$0^+_1$	5	0	0	0
	$2^+_1$	4	1	242.24	308.9
	$0^+_2$	5	0	975.96	1051.8
	$2^+_2$	4	2	707.82	825.3
	$4^+_1$	4	2	665.2	752.3
	$3^+_1$	3	3	974.8	1110.2
	$2^+_3$	4	1	1249.19	1126.9
	$4^+_2$	3	3	1183.03	1254.2
	$6^+_1$	3	3	1240	1139.3
	$0^+_3$	3	3	1218.8	1358.5
$^{109}_{45}Rh$	$(1/2)^-_1$	4	0	374.1	557.7
	$(3/2)^-_1$	4	1	568.2	634.7
	$(5/2)^-_1$	4	1	623.2	806.1
	$(3/2)^-_2$	3	2	704.9	914.3
	$(5/2)^-_2$	3	2	856.1	914.5
	$(5/2)^-_3$	4	1	926.9	1154.7
	$(3/2)^-_3$	4	1	1162.3	1040.4
	$(3/2)^-_4$	3	2	1214.3	1332.7
	$(5/2)^-_4$	3	2	1283.9	1332.9
	$(1/2)^-_2$	4	0	1631	1503.8

Table 3. The coefficients of  $T(E_2)$  used in the present work for the Ru-Rh Supermultiplets. Experimental values are taken from Refs. [26-36].

Nucleus	$q_B$	$q_f$
$^{100}Ru - ^{101}Rh$	4.27	0
$^{102}Ru - ^{103}Rh$	1.5221	0
$^{104}Ru - ^{105}Rh$	2.2782	0
$^{108}Ru - ^{109}Rh$	2.2602	0

Table 4a. B(E2) values for  $^{100}_{44}Ru$  and  $^{101}_{45}Rh$  isotopes. Experimental values are taken from Refs.[26,27] and are presented in Weisskopf units(W.u.).

Nucleus	$J_i^\pi \longrightarrow J_j^\pi$	$B(E_2(W.u.))$	
		<i>exp.</i>	<i>calc.</i>
$^{100}_{44}Rh$	$2_1^+ \longrightarrow 0_1^+$	35.6	35.6
	$0_2^+ \longrightarrow 2_1^+$	35	33.39
	$4_1^+ \longrightarrow 2_1^+$	51	55.26
	$2_2^+ \longrightarrow 2_1^+$	30.9	15.71
	$2_2^+ \longrightarrow 0_1^+$	1.9	1.9
$^{101}_{45}Rh$	$(3/2)_1^- \longrightarrow (1/2)_1^-$		2.2323
	$(5/2)_1^- \longrightarrow (1/2)_1^-$		0
	$(5/2)_2^- \longrightarrow (1/2)_1^-$		0
	$(5/2)_2^- \longrightarrow (3/2)_1^-$		0.9945
	$(5/2)_2^- \longrightarrow (5/2)_1^-$		0.0043
	$(7/2)_1^- \longrightarrow (3/2)_1^-$		5.3894
	$(9/2)_1^- \longrightarrow (5/2)_1^-$		0.9934

Table 4b. B(E2) values for  $^{102}_{44}Ru$  and  $^{103}_{45}Rh$  isotopes. Experimental values are taken from Refs.[28,29] and are presented in Weisskopf units(W.u.).

Nucleus	$J_i^\pi \longrightarrow J_j^\pi$	$B(E_2(W.u.))$	
		<i>exp.</i>	<i>calc.</i>
$^{102}_{44}Ru$	$2_1^+ \longrightarrow 0_1^+$	45.1	32.1487
	$0_2^+ \longrightarrow 2_1^+$	35	39.46
	$4_1^+ \longrightarrow 2_1^+$	66	56.34
	$2_2^+ \longrightarrow 2_1^+$	32	8.47
	$2_2^+ \longrightarrow 0_1^+$	1.14	0.11
$^{103}_{45}Rh$	$(3/2)_1^- \longrightarrow (1/2)_1^-$	36	55.98
	$(5/2)_1^- \longrightarrow (1/2)_1^-$	44	29.3311
	$(5/2)_2^- \longrightarrow (1/2)_1^-$	1.4	1.4002
	$(5/2)_2^- \longrightarrow (3/2)_1^-$	2.7	0
	$(5/2)_2^- \longrightarrow (5/2)_1^-$	4	1.34
	$(7/2)_1^- \longrightarrow (3/2)_1^-$	34	37.03
$(9/2)_1^- \longrightarrow (5/2)_1^-$	46	29.86	

Table 4c. B(E2) values for  $^{104}_{44}Ru$  and  $^{105}_{45}Rh$  isotopes. Experimental values are taken from Refs.[30,31] and are presented in Weisskopf units(W.u.).

Nucleus	$J_i^\pi \longrightarrow J_j^\pi$	$B(E_2(W.u.))$	
		<i>exp.</i>	<i>calc.</i>
$^{104}_{44}Ru$	$2_1^+ \longrightarrow 0_1^+$	57.9	35.8
	$0_2^+ \longrightarrow 2_1^+$	25	15.98
	$4_1^+ \longrightarrow 2_1^+$	83	53.36
	$2_2^+ \longrightarrow 2_1^+$	0.6	4.94
	$2_2^+ \longrightarrow 0_1^+$	2.8	2.8
$^{105}_{45}Rh$	$(3/2)_1^- \longrightarrow (1/2)_1^-$		1.37
	$(5/2)_1^- \longrightarrow (1/2)_1^-$		0.16
	$(5/2)_2^- \longrightarrow (1/2)_1^-$		0.006
	$(5/2)_2^- \longrightarrow (3/2)_1^-$		0.048
	$(5/2)_2^- \longrightarrow (5/2)_1^-$		1.32
	$(7/2)_1^- \longrightarrow (3/2)_1^-$		2.6
$(9/2)_1^- \longrightarrow (5/2)_1^-$		0.82	



Table 4d.B(E2)values for  $^{108}_{44}Ru$  and  $^{109}_{45}Rh$  isotopes.Experimental values are taken form Refs.[34,35] and are presented in Weisskopf units(W.u.).

Nucleus	$J_i^\pi \longrightarrow J_j^\pi$	$\frac{B(E_2(W.u.))}{exp. \quad calc.}$	
$^{108}_{44}Ru$	$2_1^+ \longrightarrow 0_1^+$	58	58.03
	$4_1^+ \longrightarrow 2_1^+$	102	95.3138
	$2_2^+ \longrightarrow 0_1^+$	0.5	0.5
	$6_1^+ \longrightarrow 2_2^+$	0.08	0
	$6_1^+ \longrightarrow 0_1^+$	0.004	0
	$^{109}_{45}Rh$	$(3/2)_1^- \longrightarrow (1/2)_1^-$	
$(5/2)_1^- \longrightarrow (1/2)_1^-$			0.3349
$(5/2)_2^- \longrightarrow (1/2)_1^-$			2.1831
$(5/2)_2^- \longrightarrow (3/2)_1^-$			0.0026
$(5/2)_2^- \longrightarrow (5/2)_1^-$			0.0203
$(7/2)_1^- \longrightarrow (3/2)_1^-$			0.5573
$(9/2)_1^- \longrightarrow (5/2)_1^-$			1.0983

Table 5. Parameters of Hamiltonian (30) used in the calculation of the Zn-Cu Supermultiplets. All parameters are given in keV.

Nucleus	$\mathcal{N}$	$C_s$	$C_f$	$\alpha$	$\beta'$	$\gamma$	$\sigma$	$\phi$
$^{62}Zn - ^{61}Cu$	3	0.4	0.87	889.63	0.077	15.067	217.2	10.86%
$^{64}Zn - ^{63}Cu$	4	0.51	1	946.2	0.2498	8.3402	189	8.92 %
$^{66}Zn - ^{65}Cu$	5	0.65	1	739.6	-0.136	5.947	181.92	7.05%
$^{68}Zn - ^{67}Cu$	6	0.03	0.9	988.7	2.367	-43.11	202.43	6.9 %
$^{70}Zn - ^{69}Cu$	6	0.01	0.4	914.99	1.537	-0.0468	228.18	10.23 %

Table 6a.Energy spectra for $^{62}_{30}Zn$ -  $^{61}_{29}Cu$  isotope. Experimental values are taken form Refs.[40,41]

Nuclei	$J^\pi$	$K$	$\nu_d$	$E_{exp}(keV)$	$E_{cal}(keV)$	
$^{62}_{30}Zn$	$0_1^+$	1	0	0	0	
	$2_1^+$	1	1	954	785.4	
	$2_2^+$	0	2	1804.7	2266.4	
	$4_1^+$	0	2	2186.1	1773.3	
	$0_2^+$	1	0	2330	2425.7	
	$3_1^+$	0	3	2384.5	2686.5	
	$2_3^+$	1	1	2810	2826.6	
	$4_2^+$	0	3	2743.5	2807.1	
	$2_4^+$	0	2	2890	3156	
	$2_5^+$	1	1	3470	3387.5	
	$2_6^+$	0	2	3640	3484.7	
	$^{61}_{29}Cu$	$(3/2)_1^-$	1	0	0	0
		$(1/2)_1^-$	0	1	475.1	524.3
		$(5/2)_1^-$	0	1	970.06	726.1
$(7/2)_1^-$		0	1	1310.55	1431.6	
$(5/2)_2^-$		0	2	1394.2	1855.7	
$(7/2)_2^-$		0	2	1732.61	1961.3	
$(5/2)_3^-$		0	2	1904.18	1855.7	
$(7/2)_3^-$		0	2	1942.49	1961.3	
$(1/2)_2^-$		0	2	2088.86	1734.7	
$(5/2)_4^-$		0	1	2203.4	2415.81	
$(9/2)_1^-$		0	2	2295.09	2096.9	

Table 6b. Energy spectra for  $^{64}_{30}\text{Zn}$ - $^{63}_{29}\text{Cu}$  isotope. Experimental values are taken from Refs.[42,43]

Nuclei	$J^\pi$	$K$	$\nu_d$	$E_{exp}(\text{keV})$	$E_{cal}(\text{keV})$	
$^{64}_{30}\text{Zn}$	$0^+_1$	2	0	0	0	
	$2^+_1$	1	1	991.54	1040.878	
	$2^+_2$	1	2	1799.41	1406.2	
	$4^+_1$	1	2	2306.68	2487.7	
	$3^+_1$	1	1	2979.81	2820.4	
	$2^+_3$	1	1	2793.7	2770.4	
	$4^+_2$	0	3	2736.6	2887.2	
	$2^+_4$	1	2	3005.72	3170.3	
	$2^+_5$	0	4	3094.6	2820.4	
	$0^+_2$	2	0	1910.3	1725.6	
	$0^+_3$	2	0	2609.45	2324.5	
	$4^+_3$	0	3	3078.43	2887.2	
	$3^+_2$	0	3	3094.6	2820.4	
	$^{63}_{29}\text{Cu}$	$(3/2)^-_1$	1	0	0	0
		$(1/2)^-_1$	1	1	669.67	724.4
		$(5/2)^-_1$	1	1	962.1	1295.6
$(7/2)^-_1$		1	1	1327.01	1105.4	
$(5/2)^-_2$		0	2	1412.05	1844.4	
$(3/2)^-_1$		1	1	1547.05	1404.1	
$(7/2)^-_2$		0	2	1904.5	1861.61	
$(7/2)^-_3$		0	2	2092.6	2204.5	
$(3/2)^-_2$		1	0	2011.25	1802	
$(1/2)^-_2$		0	2	2062.23	1777.7	
$(9/2)^-_1$		0	2	2207.88	2179.6	
$(5/2)^-_3$		0	2	2336.58	2595.9	

Table 6c. Energy spectra for  $^{66}_{30}\text{Zn}$ - $^{65}_{29}\text{Cu}$  isotope. Experimental values are taken from Refs.[44,45]

Nuclei	$J^\pi$	$K$	$\nu_d$	$E_{exp}(\text{keV})$	$E_{cal}(\text{keV})$	
$^{66}_{30}\text{Zn}$	$0^+_1$	2	0	0	0	
	$2^+_1$	2	1	1039.39	1069.4	
	$2^+_2$	1	2	1872.94	2245.9	
	$4^+_1$	1	2	2451.13	2660.1	
	$2^+_3$	2	1	2780.55	2772.5	
	$4^+_2$	1	3	2765.69	2913.6	
	$2^+_4$	1	2	2938.45	2985.5	
	$0^+_2$	2	0	2372.53	2524.7	
	$0^+_3$	2	0	3030	3262.3	
	$4^+_3$	1	3	3077.93	3280.8	
	$^{65}_{29}\text{Cu}$	$(3/2)^-_1$	2	0	0	0
		$(1/2)^-_1$	1	1	770.64	794.4
		$(5/2)^-_1$	1	1	1115.556	1523
		$(7/2)^-_1$	1	1	1481.83	1564.6
$(5/2)^-_2$		1	2	1623.43	1736.1	
$(3/2)^-_2$		1	1	1725	1922.9	
$(7/2)^-_2$		2	1	2094.34	2208.1	
$(7/2)^-_3$		0	2	2092.6	2204.5	
$(3/2)^-_3$		2	0	2329.05	2449.2	
$(1/2)^-_2$		1	2	2212.84	2118.9	
$(5/2)^-_3$		1	2	2107.44	2365.5	
$(5/2)^-_4$	1	1	2532.04	2691.6		

Table 6d. Energy spectra for  $^{68}_{30}\text{Zn}$ - $^{67}_{29}\text{Cu}$  isotope. Experimental values are taken from Refs.[46,47]

Nuclei	$J^\pi$	$K$	$\nu_d$	$E_{exp}(\text{keV})$	$E_{cal}(\text{keV})$
$^{68}_{30}\text{Zn}$	$0_1^+$	3	0	0	0
	$2_1^+$	2	1	1077.37	1183.3
	$2_2^+$	2	2	1883.14	1989.8
	$4_1^+$	2	2	2417.44	2379.2
	$2_3^+$	2	1	2338.29	2470
	$4_2^+$	1	3	2955.9	2893.5
	$2_4^+$	2	2	2821.58	2978.5
	$0_2^+$	3	0	1655.94	1627.5
	$0_3^+$	3	0	3102.45	3213.6
	$3_1^+$	1	3	3009.2	3238.4
$^{67}_{29}\text{Cu}$	$(3/2)_1^-$	2	0	0	0
	$(1/2)_1^-$	2	1	2272	2212.6
	$(3/2)_2^-$	2	1	1937.1	2070
	$(3/2)_2^-$	1	1	1725	1922.9
	$(3/2)_3^-$	2	0	2272	2564.8
	$(1/2)_2^-$	1	2	2623.1	2707.9
	$(3/2)_4^-$	1	2	2623.1	2595.1
	$(3/2)_5^-$	2	1	2680.1	3058.7
	$(1/2)_3^-$	2	1	2841.1	3201.3
	$(3/2)_6^-$	1	3	2841.1	3090.4

Table 6e. Energy spectra for  $^{70}_{30}\text{Zn}$ - $^{69}_{29}\text{Cu}$  isotope. Experimental values are taken from Refs.[48,49]

Nuclei	$J^\pi$	$K$	$\nu_d$	$E_{exp}(\text{keV})$	$E_{cal}(\text{keV})$	
$^{70}_{30}\text{Zn}$	$0_1^+$	3	0	0	0	
	$2_1^+$	2	1	884.8	952.3	
	$2_2^+$	2	2	1759.1	2074	
	$4_1^+$	2	2	1786.5	1923.1	
	$2_3^+$	2	1	1957.7	2389.6	
	$4_2^+$	1	3	2693.6	2458.6	
	$2_4^+$	2	2	2538	2464.3	
	$0_2^+$	3	0	1068.3	1163.7	
	$0_3^+$	3	0	2140.4	2016.9	
	$3_1^+$	1	3	2949.6	2838.1	
	$2_6^+$	2	1	3635	3438.1	
	$0_4^+$	1	3	3680	3465.2	
	$2_7^+$	2	2	3710.6	3904.6	
	$^{69}_{29}\text{Cu}$	$(3/2)_1^-$	2	0	0	0
		$(1/2)_1^-$	2	1	1096	1540.4
$(7/2)_1^-$		2	1	1710.8	1539.7	
$(7/2)_2^-$		1	2	1870	2007.7	

Table 7. The coefficients of  $T(E_2)$  used in the present work for the Ru-Rh Supermultiplets..Experimental values are taken form Refs. [40-49] .

Nucleus	$q_B$	$q_f$
$^{61}\text{Cu} - ^{62}\text{Zn}$	2.4197	-0.9731
$^{63}\text{Cu} - ^{64}\text{Zn}$	2.1278	-0.28
$^{65}\text{Cu} - ^{66}\text{Zn}$	8.775	0
$^{67}\text{Cu} - ^{68}\text{Zn}$	4.9527	0
$^{69}\text{Cu} - ^{70}\text{Zn}$	7.7603	0

Table 8a. B(E2)values for  $^{61}\text{Cu}$  and  $^{62}\text{Zn}$  isotopes. Experimental values are taken form Refs.[40,41]and are presented in Weisskopf units(W.u.).

Nucleus	$J_i^\pi \longrightarrow J_j^\pi$	$B(E_2(\text{W.u.}))$	
		<i>exp.</i>	<i>calc.</i>
$^{61}\text{Cu}$	$2_1^+ \longrightarrow 0_1^+$	16.8	15.3989
	$2_2^+ \longrightarrow 2_1^+$	18	17.2585
	$4_1^+ \longrightarrow 2_1^+$	26	25.7274
	$2_2^+ \longrightarrow 0_1^+$	0.32	0.14
	$3_1^+ \longrightarrow 2_2^+$	110	45.21
	$3_1^+ \longrightarrow 2_1^+$	0.5	0.5466
$^{62}\text{Zn}$	$(5/2)_1^- \longrightarrow (1/2)_1^-$	17	9.006
	$(5/2)_1^- \longrightarrow (3/2)_1^-$	7.2	1.4164
	$(7/2)_2^- \longrightarrow (5/2)_1^-$	0.03	0
	$(7/2)_2^- \longrightarrow (3/2)_1^-$	18	20.4437
	$(3/2)_2^- \longrightarrow (3/2)_1^-$	1.5	1.1757

Table 8b. B(E2)values for  $^{64}\text{Zn}$  and  $^{63}\text{Cu}$  isotopes. Experimental values are taken form Refs.[42,43]and are presented in Weisskopf units(W.u.).

Nucleus	$J_i^\pi \longrightarrow J_j^\pi$	$B(E_2(\text{W.u.}))$	
		<i>exp.</i>	<i>calc.</i>
$^{64}\text{Zn}$	$2_1^+ \longrightarrow 0_1^+$	20	28.9867
	$0_2^+ \longrightarrow 2_1^+$	0.057	3.2783
	$4_1^+ \longrightarrow 2_1^+$	12.2	9.7
	$2_2^+ \longrightarrow 2_1^+$	39	35.186
	$2_2^+ \longrightarrow 0_1^+$	0.24	0.92
	$0_3^+ \longrightarrow 2_2^+$	1.3	0.00
$^{63}\text{Cu}$	$(1/2)_1^- \longrightarrow (3/2)_1^-$	15.2	15.7863
	$(5/2)_1^- \longrightarrow (3/2)_1^-$	15.7	12.7599
	$(7/2)_1^- \longrightarrow (3/2)_1^-$	12.7	11.05
	$(5/2)_2^- \longrightarrow (1/2)_1^-$	6	5.3356
	$(5/2)_2^- \longrightarrow (3/2)_1^-$	1	0.002
	$(3/2)_2^- \longrightarrow (3/2)_1^-$	3.7	0.00
	$(7/2)_2^- \longrightarrow (3/2)_1^-$	1.4	0.94

Table 8c. B(E2)values for  $^{66}\text{Zn}$  and  $^{65}\text{Cu}$  isotopes. Experimental values are taken from Refs.[44,45]and are presented in Weisskopf units(W.u.).

Nucleus	$J_i^\pi \longrightarrow J_j^\pi$	$\frac{B(E_2(W.u.))}{\text{exp.} \quad \text{calc.}}$	
$^{66}\text{Zn}$	$2_1^+ \longrightarrow 0_1^+$	17.5	8.0597
	$2_2^+ \longrightarrow 2_1^+$	330	330.3182
	$2_2^+ \longrightarrow 0_1^+$	0.032	0.032
	$4_1^+ \longrightarrow 2_1^+$	18	14.7453
	$2_3^+ \longrightarrow 2_1^+$	0.13	0
	$2_3^+ \longrightarrow 0_1^+$	0.54	4.6768
$^{65}\text{Cu}$	$(1/2)_1^- \longrightarrow (3/2)_1^-$		0.003
	$(5/2)_1^- \longrightarrow (3/2)_1^-$		31.5248
	$(7/2)_1^- \longrightarrow (5/2)_1^-$		0.001
	$(5/2)_2^- \longrightarrow (1/2)_1^-$		0.3517
	$(5/2)_2^- \longrightarrow (3/2)_1^-$		5.5851

Table 8e. B(E2)values for  $^{68}\text{Zn}$  and  $^{67}\text{Cu}$  isotopes. Experimental values are taken from Refs.[46,47]and are presented in Weisskopf units(W.u.).

Nucleus	$J_i^\pi \longrightarrow J_j^\pi$	$\frac{B(E_2(W.u.))}{\text{exp.} \quad \text{calc.}}$	
$^{68}\text{Zn}$	$2_1^+ \longrightarrow 0_1^+$	14.69	9.61
	$4_1^+ \longrightarrow 2_1^+$	10.8	7.7922
	$2_2^+ \longrightarrow 0_1^+$	16	8.425
	$0_2^+ \longrightarrow 2_1^+$	5.5	3.366
	$2_2^+ \longrightarrow 0_2^+$	16	8.425
	$2_2^+ \longrightarrow 2_1^+$	28.6	29.683
$^{67}\text{Cu}$	$(1/2)_1^- \longrightarrow (3/2)_1^-$		0.058
	$(5/2)_1^- \longrightarrow (3/2)_1^-$		0.3646
	$(7/2)_1^- \longrightarrow (5/2)_1^-$		0.00
	$(5/2)_2^- \longrightarrow (1/2)_1^-$		0.6664
	$(5/2)_2^- \longrightarrow (3/2)_1^-$		3.2829

Table 8d. B(E2)values for  $^{70}\text{Zn}$  and  $^{69}\text{Cu}$  isotopes. Experimental values are taken from Refs.[48,49]and are presented in Weisskopf units(W.u.).

Nucleus	$J_i^\pi \longrightarrow J_j^\pi$	$\frac{B(E_2(W.u.))}{\text{exp.} \quad \text{calc.}}$	
$^{70}\text{Zn}$	$2_1^+ \longrightarrow 0_1^+$	16.5	12.3661
	$0_2^+ \longrightarrow 2_1^+$	37.3	37.1785
	$2_2^+ \longrightarrow 2_1^+$	69	42.23
	$2_2^+ \longrightarrow 0_1^+$	2.4	1.275
	$2_4^+ \longrightarrow 0_1^+$	0.15	0.8133
$^{69}\text{Cu}$	$(1/2)_1^- \longrightarrow (3/2)_1^-$		0.145
	$(5/2)_1^- \longrightarrow (3/2)_1^-$		1.002
	$(7/2)_1^- \longrightarrow (5/2)_1^-$		0.002
	$(5/2)_2^- \longrightarrow (1/2)_1^-$		0.328
	$(5/2)_2^- \longrightarrow (3/2)_1^-$		0.418

Table 9. Comparison of key observable in Ru isotopes with the E(5) symmetry.

Nucleus	$R_{\frac{4}{2}}$	$C_s$	$\frac{E(0_2^+)}{E(2_1^+)}$	$B\left(\frac{E2;4_1^+ \rightarrow 2_1^+}{E2;2_1^+ \rightarrow 0_1^+}\right)$	$B\left(\frac{E2;0_2^+ \rightarrow 2_1^+}{E2;2_1^+ \rightarrow 0_1^+}\right)$
E(5)	2.19	-	3.03	1.68	0.68
$^{100}\text{Ru}$	2.24	0.38	2.5544	1.55	0.9379
$^{102}\text{Ru}$	2.37	0.23	1.6227	1.7524	1.2274
$^{104}\text{Ru}$	2.32	0.54	3.18	1.49	0.446
$^{106}\text{Ru}$	2.526	0.34	3.38	-	-
$^{108}\text{Ru}$	2.435	0.65	3.4	1.64	-

Table 10. Comparison of key observable in Zn isotopes with the E(5) symmetry.

Nucleus	$R_{\frac{4}{2}}$	$C_s$	$\frac{E(0_2^+)}{E(2_1^+)}$	$B\left(\frac{E2;4_1^+ \rightarrow 2_1^+}{E2;2_1^+ \rightarrow 0_1^+}\right)$	$B\left(\frac{E2;0_2^+ \rightarrow 2_1^+}{E2;2_1^+ \rightarrow 0_1^+}\right)$
E(5)	2.19	-	3.03	1.68	0.68
$^{62}\text{Zn}$	2.257	0.51	3.088	1.55	0.9379
$^{64}\text{Zn}$	2.391	0.4	1.657	1.7524	1.2274
$^{66}\text{Zn}$	2.48	0.65	2.36	1.49	0.446
$^{68}\text{Zn}$	2.014	0.03	1.375	-	-
$^{70}\text{Zn}$	2.0194	0.01	1.22	1.64	-

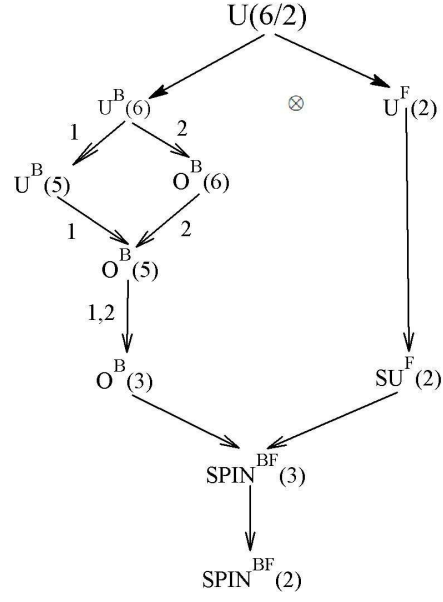


FIG. 1. The lattice of algebras in the  $U(6/2)$  supersymmetry scheme.

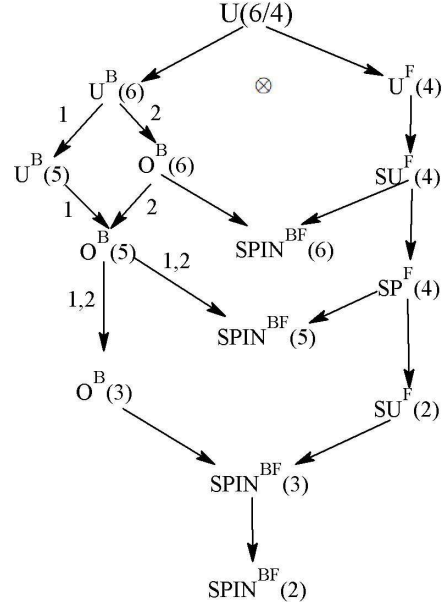


FIG. 2. The Lattice of algebras in the  $U(6/4)$  supersymmetry scheme.

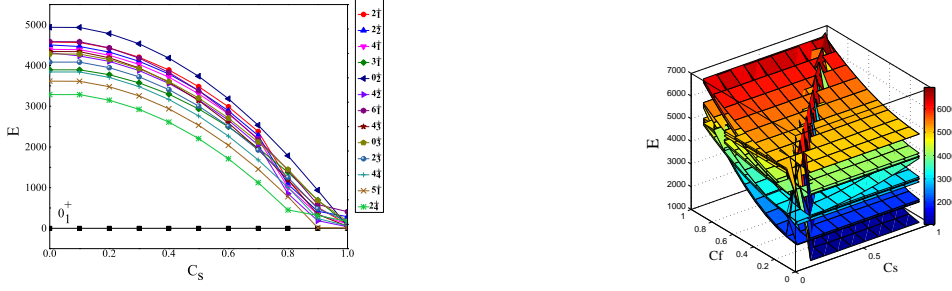


FIG. 3. Energy levels as a function of  $C_s$  control parameter for a even-even nuclei (left panel) and for odd-A nuclei as a function of the  $C_s$  and  $C_f$  control parameters(right panel) in the Hamiltonian (27) for  $N = 10$  bosons with  $\alpha = 1000$ ,  $\beta = 3.14$ ,  $\delta = -5.26$ ,  $\gamma = 0.0439$ .

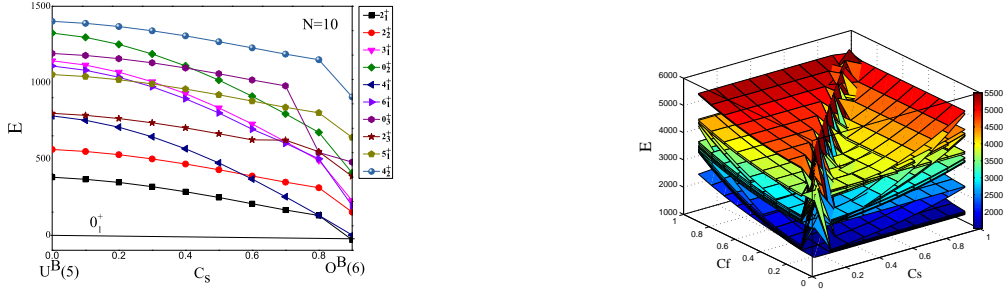


FIG. 4. Energy levels as a function of  $C_s$  control parameter for a even-even nuclei (left panel) and for odd-A nuclei as a function of the  $C_s$  and  $C_f$  control parameters(right panel) in the Hamiltonian (30) for  $N = 10$  bosons with  $\alpha = 1000$ ,  $\beta' = -1.29$ ,  $\gamma = 6.05$ .

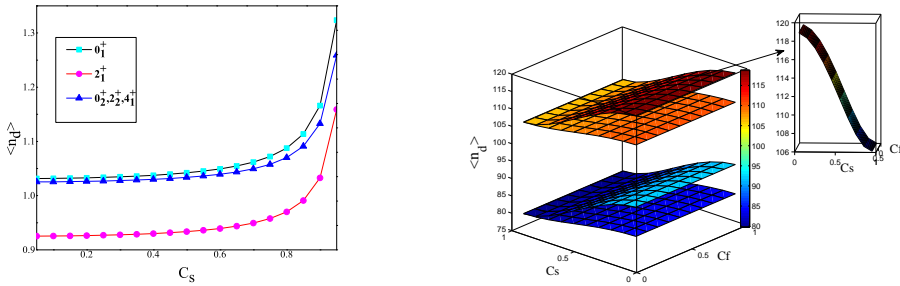


FIG. 5. The expectation values of the  $d$ -boson number operator for the lowest states as a function of  $C_s$  control parameter for an even-even nuclei (left panel) and for odd-A nuclei as a function of the  $C_s$  and  $C_f$  control parameters(right panel) for  $j=1/2$ .



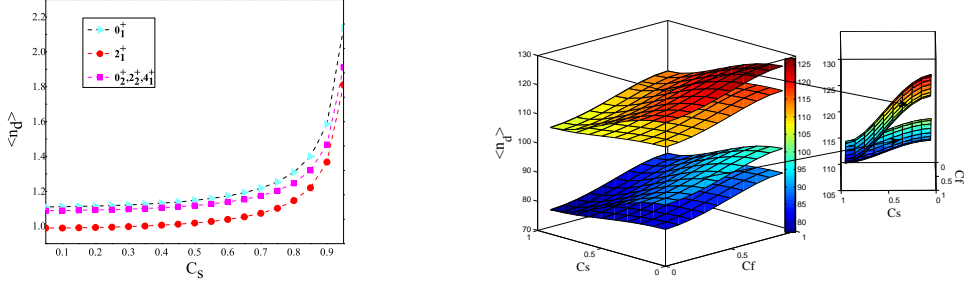


FIG. 6. The expectation values of the  $d$ -boson number operator for the lowest states as a function of  $C_s$  control parameter for an even-even nuclei (left panel) and for odd-A nuclei as a function of the  $C_s$  and  $C_f$  control parameters (right panel) for  $j=3/2$ .

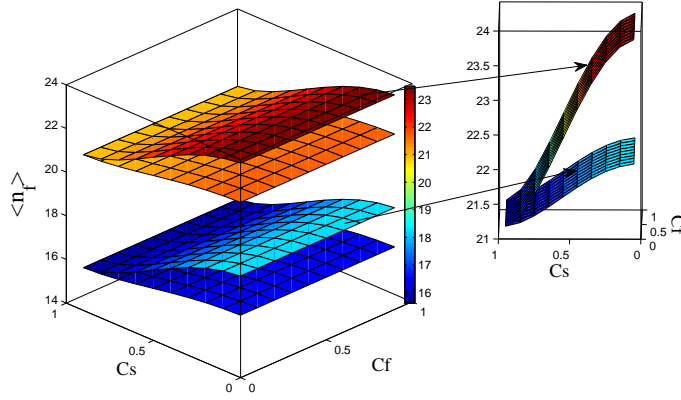


FIG. 7. The expectation values of the fermion number operator for odd-A nuclei for the lowest states as a function of  $C_s$  and  $C_f$  control parameters.

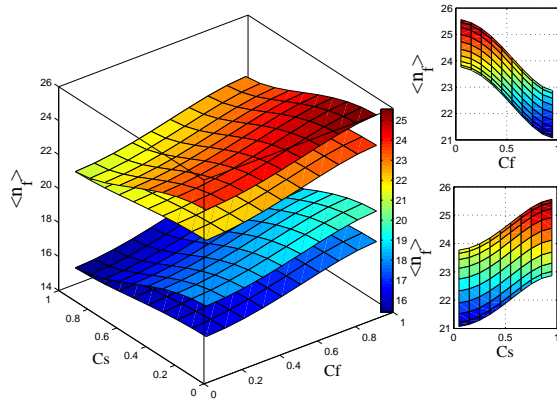


FIG. 8. The expectation values of the fermion number operator for odd-A nuclei for the lowest states as a function of  $C_s$  and  $C_f$  control parameters.

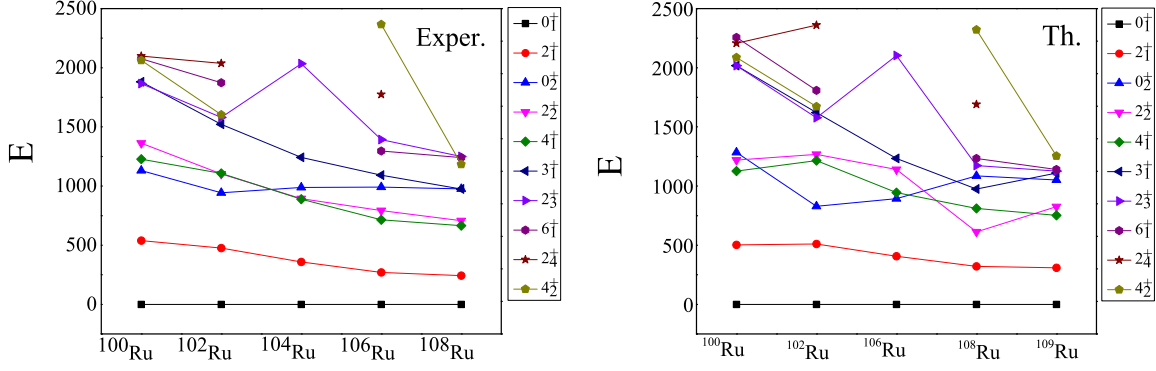


FIG. 9. Comparison between calculated and experimental spectra of positive parity states in Ru Isotopes. The parameters of the calculation are given in Tables 2. In the experimental spectra, taken from [26, 28, 30, 32, 34, 36].

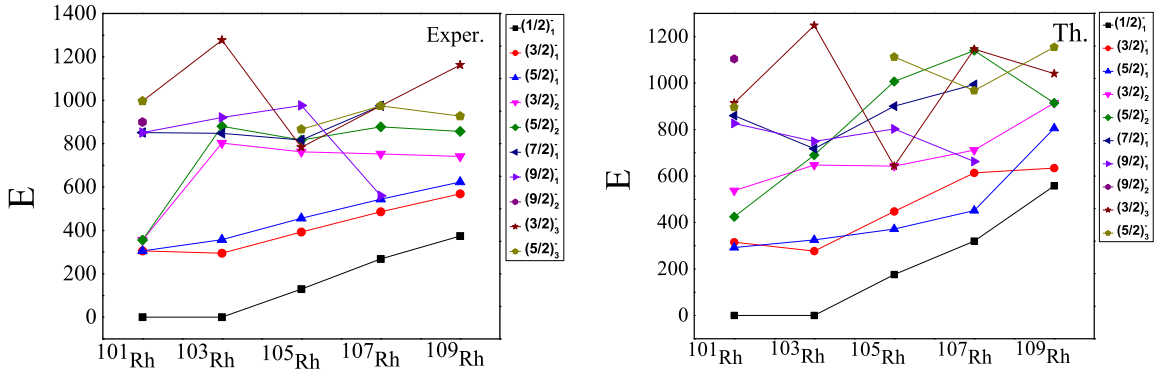


FIG. 10. Comparison between calculated and experimental spectra of negative parity states in Rh Isotopes. The parameters of the calculation are given in Tables 1. In the experimental spectra, taken from [27, 29, 31, 33, 35, 36].

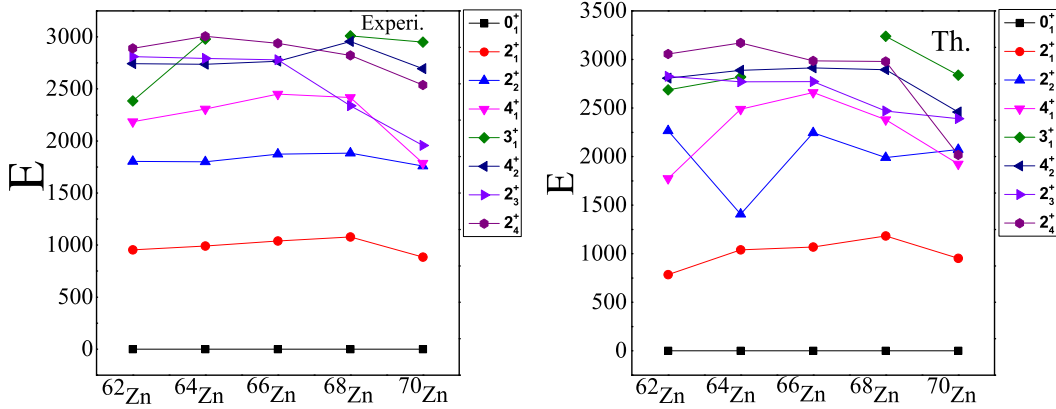


FIG. 11. Comparison between calculated and experimental spectra of positive parity states in Zn Isotopes. The parameters of the calculation are given in Tables 2. In the experimental spectra, taken from [36, 41, 43, 45, 47, 49].

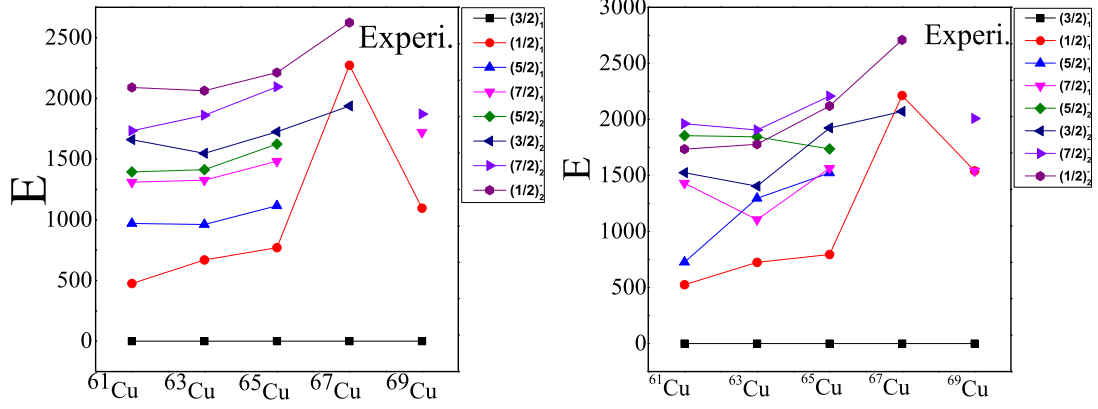


FIG. 12. Comparison between calculated and experimental spectra of negative parity states in Cu Isotopes. The parameters of the calculation are given in Tables 1. In the experimental spectra, taken from [36, 40, 42, 44, 46, 48].

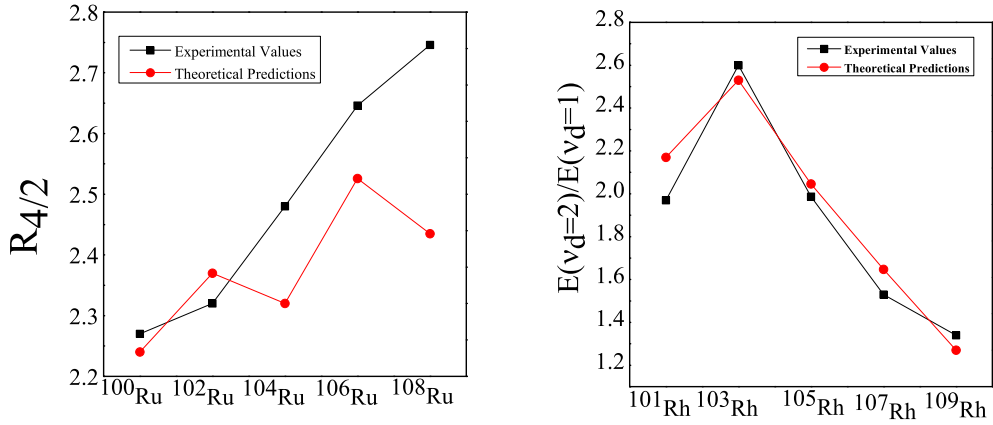


FIG. 13.  $(E(\nu_d = 2))/(E(\nu_d = 1))$  prediction values for Ru and Rh Isotopes. In the experimental spectra, taken from [26, 28, 30, 32, 34, 36]

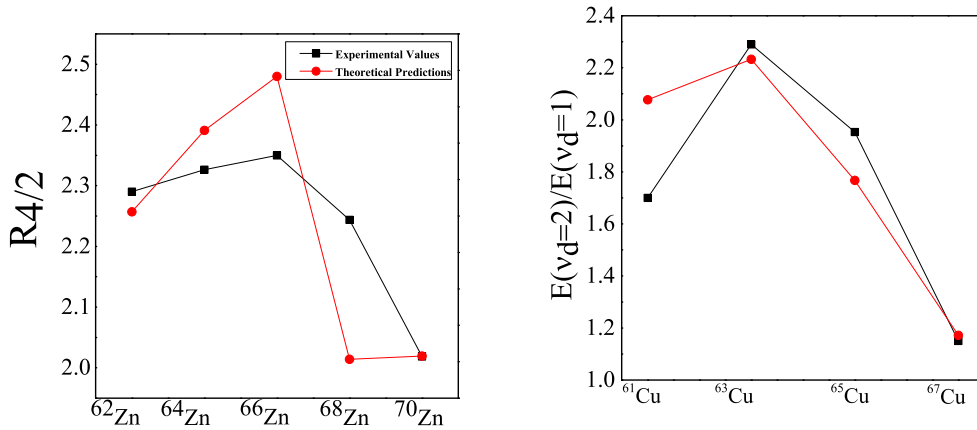


FIG. 14.  $(E(\nu_d = 2))/(E(\nu_d = 1))$  prediction values for Zn and Cu Isotopes. In the experimental spectra, taken from [27, 29, 31, 33, 35, 36]

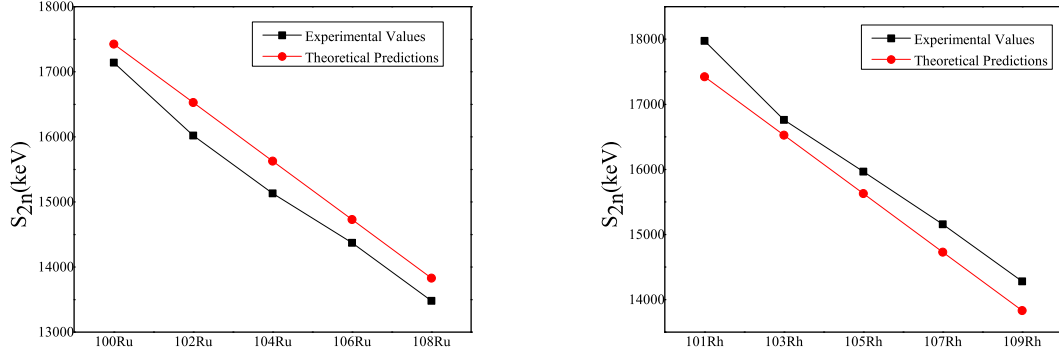


FIG. 15. A comparison between theoretical and experimental two neutron separation energies,  $S_{2n}$  (in keV) for Ru isotopes (left panel) and Rh isotopes (right panel). Experimental data from [36].

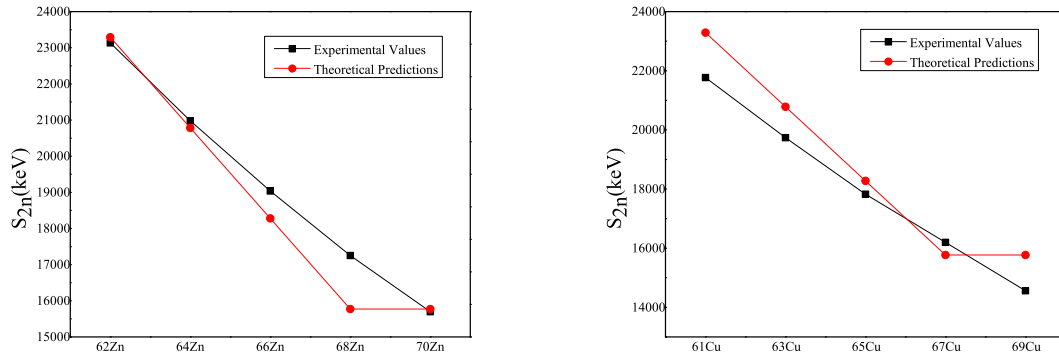


FIG. 16. A comparison between theoretical and experimental two neutron separation energies,  $S_{2n}$  (in keV) for Zn isotopes (left panel) and Cu isotopes (right panel). Experimental data from [36].

